Republic of Iraq
Ministry of Higher Education
and Scientific Research
University of Babylon
College of Science
Department of Physics

Influence of Structures of Organometallic Molecular Junction on Electrical and Thermal Transport

A Thesis
Submitted to the Physics Department, College of Science,
University of Babylon in Partial Fulfillment of the Requirements for the Degree of Master of Science in Physics

By

Ayed Fadhil Mushir Mashal

B.Sc. physics-University of Babylon/(2011)

Supervised by

Assist. Prof. Dr. Rawaa Mezher Obaid

Assist. Prof. Dr. Mohsin Kadhim Abed

2021 A.D

1443 H.D

بسم الله الرحمن الرحيم

﴿يَرْفَعِ اللَّهُ الَّذِينَ آمَنُوا
مِنكُمْ وَالَّذِينَ أُوتُوا الْعِلْمَ
دَرَجَاتٍ وَاللَّهُ بِمَا تَعْمَلُونَ
خَبِيرٌ﴾

صدق الله العلي العظيم

سورة المجادلة (الاية ١١)

Supervisors Certification

We certify that this thesis is titled ((**Influence of Structures of Organaometallic Molecular junctions on Electrical and Thermal Transport)**) will be prepared by (**Ayed Fadhil Mushir Meshal**) under our supervisions in partial fulfillment of the requirements for pratical degree Master thesis in (Nanoelectronic).

Signature:
Supervisor: Dr. Rawaa M.Obaid
Title: Assistant Professor
Address: Department of physics- College of science- University of Babylon.

Signature:
Supervisor: Dr. Mohsin K. Abed
Title: Assistant Professor
Address: Department of physics- College of science- University of Babylon.

Data: / /2021

Certification of the Head of the Department

In view of the available recommendation , I forward this thesis for debate by the Examining Committee.

Signature:

Name : Dr. Abdulazeez O. Mousa Al-Ogaili

Title: Prof.

Address: Head of Department of physics – College of science – University of Babylon.

Data: / / 2021

Examining Committee Certificate

We certify that we have read this thesis entitled **"Influence of Structures of Organometallic Molecular Junction on Electrical and Thermal Transport"** and, as an examining Committee, examined the student **"Ayed Fadhil Mushir Mashal"** in its content and that, in our opinion it meets the standards of a thesis for the degree of Master of Science Physics.

Signature:
Name: Dr. Nidhal Mohammed O. Al Shareefi
Title: Assistant Professor
Address: Department of Physics-College of Science-University of Babylon
Date : / / 2021
(Chairman)

Signature:
Name: Dr. Qusiy H. Al-Galiby
Title: Assistant Professor
Address: Department of Physics-College of Education-University of Al-Qadisiyah
Date : / / 2021
(Member)

Signature:
Name: Dr. Shurooq Sabah Abid Al-Abbas
Title: Assistant Professor
Address: Department of Physics-College of Education for Pure Science- University of Babylon
Date: / / 2021
(Member)

Signature:
Name: Dr. Rawaa Mezher Obaid
Title: Asst. Professor
Address: Department of Physics- College of Science- University of Babylon
Date: / / 2021
(Member and Supervisor)

Signature:
Name: Dr. Mohsin Kadhim Abed
Title: Asst. Professor
Address: Department of Physics- College of Science -University of Babylon
Date: / / 2021
(Member and Supervisor)

Approved by the College committee on graduate studies

Signature:
Name: Dr. Enas M . Al-Robayi
Title: Professor
Address: Dean of the College of Science-University of Babylon
Date: / / 2021

Acknowledgments

Praise is to ***Allah,*** Mercy and peace are to the Prophet ***Mohammad*** and ***his Relatives*****.**

First, I would like to thank my supervisor, ***Dr. Rawaa Mezher Obaid and Dr. Mohsin K. Al-Khaykanee*** for suggesting the topic of this thesis, suggestions and continuous encouragement throughout the research work.

I am also thankful to and all ***my family*** for their perpetual encouragement and support.

A word of thanks is due to the ***Head and Staff Members*** of the Department of Physics, the College of Science and the ***Dean*** of the College of science of University of Babylon.

Finally, I wish I have a word better than thanks to express my feeling to ***my Friends*** for their understanding, never-ending encouragement, and support throughout this work.

Ayed

Dedication

To:

My family

My teachers

My close friends

My beloved country Iraq

and

Every one who has helped me ...

Ayed

Summary

Molecular structures of a series of metal-complexes molecules of bipyrimdine have interesting features in various applications such as industrial and scientific. The transition through metal complexes at molecular structures has a significant role in the metal-bridges interactions. Hence, the bipyrimdine's complex molecules were used to show the effect of the metal atoms on the electronics, electrical, and thermal properties and to identify the π-conjugated system in all attempts before/ or after replaced one carbon with nitrogen atoms in one or two the pyridine rings.

The Gaussian 09 package, SIESTA code, and GOLLUM code programs were used in our calculations. The results showed that the energy gap decreased significantly with the type of metal atoms, which appear in electronic applications at various LUMO-HOMO energy gaps. Moreover, the findings showed the appearance of the IR and UV-Vis spectrum, which have viewed different behavior with the type of metal complexes. The electrical and thermal results have confirmed the effect of metal-complexes center atoms in the transmission and Seebeck coefficients.

From the position of the Fermi energy ($E-E_F=0$ eV), the conductance and the Seebeck coefficient values are determined, and thus the specificity figure of merit ZT_e was computed. Therefore, we found the ZT_e be a high value for bipyridine molecule about 1.7, which is several order of magnitude higher than of the set molecules. Whereas a low value of ZT_e for Cr-metal- molecule.

Contents

List of Symbols and abbreviations

Symbol	*Description*
σ	Bonding Sigma Molecular Orbitals
σ^*	Antibonding Sigma Molecular Orbitals
π	Bonding Pi Molecular Orbitals
π*	Antibonding Pi Molecular Orbitals
LCAO	Linear combination of atomic orbitals
Bpy	Bipyridine molecules
Bpyrim	Bipyrimdine molecules
MM	Molecular Mechanics
SE	Semiempirical Methods
V (r, t)	Potential Energy
$\hat{H}$	The Hamiltonian Operator
∇^2	Laplacian operator
ħ	The reduced Planck constant (h/2π)
$\psi\ (\vec{r}, \vec{R})$	The Total Wave Function
E_{tot}	The Total Energy
m_e	Electronic Mass
$\hat{T}_e$	The Electronic Kinetic Energy Operator
$\hat{T}_n$	The Nuclear Kinetic Energy Operator
$\hat{V}_{ne}$	The Attractive Interactions between Nuclei and Electrons Operator
$\hat{V}_{ee}$	The Repulsive Electron– Electron Interactions Operator
$\hat{V}_{nn}$	The Repulsive Nucleus- Nucleus Interactions Operator
$Z_{A,B}$	The Atomic Number of Atoms A and B
m_A	The Mass of Atom A
r_{AB}	The Distance between Nuclei A and B
r_{iA}	The Distance between Nucleus A and Electron i
r_{ij}	The Distance between Electrons i and j
$\hat{H}_e$	The Electronic Hamiltonian Operator
ψ_e	The Electronic Wave Function
E_e	The Electronic Energy
V_{ext}	The External Potential
E_0	The Ground-State Energy
B3LYP	Beckel three parameters Lee-Yang-Par

Symbol	*Description*
$\rho(r)$	Electron Density
E_{xc}	Exchange-correlation energy
V_{XC}	Exchange-correlation potential
LDA	Local density approximation
L(S)DA	Local (Spin) Density Approximation
GGA	The Generalized Gradient Approximation
$\rho_0(x,y,z)$	The Ground State Electron Density
$F_{HK}[\rho]$	Hohenberg-Kohn Operator
ψ_i	Wave Function Molecular Orbitals
GTO's	Gaussian Type Orbitals
STO's	Slater Type Orbitals
ξ	Orbital exponent
MO	Molecular orbital
FMO	Frontier molecular orbitals
HOMO	Highest Occupied Molecular Orbital
LUMO	Lowest Unoccupied Molecular Orbital
E_g	Energy Gap
α,β	Spin up and spin down
K	Chemical Potential
X	Electronegativity
ω	Electrophilicity index
H	Chemical Hardness
Y_{lm}	Spherical harmonic
SZ	Single-zeta
VDZ	The valence double-zeta (VDZ) basis set
VTZ	The valence triple-zeta(VTZ) basis set
DFT	Density Functional Theory
HF	Hartree-Fock
IR	Infrared Ray
UV	Ultra-Violet
UV-Vis	Ultraviolet-Visible
Cr	Chromium Metal
Mo	Molybdenum Metal
W	Tungsten Metal
SCF	Self-Consistent Field
KS	Kohn–Sham

Symbol	*Description*
DOS	Density of State
T(E)	Transmission Coefficient
S	Seebeck Coefficients
G/G◦	The room temperature conductance of GR1
G◦	The conductance through the two contacting pyramids
G09	Gaussian 2009
SIESTA	Spanish Initiative for Electronic Simulations with Thousands of Atoms

List of Figures

List of Tables

Chapter one

Introduction and Literature Review

1.1 Introduction

Molecular electronics is one of the new branches of science that is to understand the idea of using organometallic single-molecules as functional units in electronic devices, which views an alternative to present silicon-based technologies. The key role of minute size and design of molecular structures renders recently single-molecules functional units in electronics devices, chemistry, protein science, biochemistry, and industrial applications [1]. In the past decades, single-molecule has become more important and interesting due to its use in electronic elements in circuitry and the control of bandgap energy comprising semiconductor technology. Designing and construction of organometallic molecules is an active field of research due to their possible application to information technology, in particular, the form of molecular-scale electronics devices, the biological environment, and complementing all views of the transition of metal complexes applications as in medicine. The study of molecular-scale electronics has been driven by fundamental interest and by potential practical applications The highly interdisciplinary subject is a meeting place for synthetic chemists, physical chemists, and experimental physicists[2].

Organic or organometallic compounds might potentially replace silicon in laptops and mobile devices. Especially compared to silicon-based electronic devices, molecular-scale electronics have various advantages. Firstly, the smaller size of molecular structures, which can be as small as 1-2 nanometers in length, may lead to faster device performance, perhaps exceeding the limit of silicon-based circuit integration. At the nanoscale, silicon circuits start to become inefficient as they leak current and heat. The term “nano” refers to a length scale of approximately 10^{-9} or one billionths of a meter. Second, there is a huge diversity in the types of molecular structures that chemists can make, which means that the properties of molecules can be rationally and systematically changed [3].

This has led to the discovery of new effects and phenomena that do not occur in traditional materials such as silicon. Also, for industrial applications, some molecules can be readily synthesized in bulk quantities offering low-cost manufacturing potential [4].

1.2 Nano Scale

Nanoscale science involves understanding the fundamental interactions of physical systems confined to nanoscale dimensions, and when the matter is controlled at the nanoscale, fundamental properties of things like temperature, electricity, magnetism, and chemical reactions can change completely. The laws of classical physics describe our cosmic universe, the motions of the planets, the trajectory of a baseball, and the behavior of things we experience every day. However, the laws of quantum mechanics apply in the nano-world. The operation of computer chips in present-day computers can be explained by the laws of classical electron flow; but when electrons are confined to nanoscale dimensions, they behave according to the laws of quantum mechanics. Consequently, future chips made with nanoscale dimensions (called q-bits) will process information differently and lead to computers with new logic and functionality. Similarly, materials formed from nanoscale grains can exhibit dramatic property improvements, and drugs at the nanoscale can become more effective with fewer side effects. Nanoscale science strives to understand these changes [5].

Nanoscale technology refers to our ability to utilize our understanding of nanoscale science to fabricate products with new properties and capabilities. To fully realize the possibilities, it becomes crucial to understand quantum interactions at the nanoscale; to be able to see nanoscale structures; and to be able to form, manipulate, and even connect nanostructures.

Now scientists have learned to manipulate individual molecules or fabricate nanowires and connect them for information processing (so-called “bottom-up”

technology). These technologies will have a dramatic effect on future advances in medicine, biology, and energy, as well as in materials science, semiconductor devices, and computer technology[6].

Recently, new insights in the field of nanoscience have been obtained from the application of fundamental modeling techniques such as density functional theory (DFT), and molecular dynamics. Advances in computer technology have led to an increase in computational capability which has made possible the modeling and simulation of complex systems with many degrees of freedom[5,7].

1.3 Molecular Electronics

Molecular electronics is presented as the field of science that investigates the electronic transport properties of systems in which individual molecules are used as a basic building block. The dimensions of some molecular systems are a few nanometers, and therefore molecular electronic should be viewed as a subfield of nanotechnology [8]. In terms of potential technology, molecular electronics is based on the bottom-up approach where the idea is to assemble specific and designed molecules to form more complex structures, active components, and connecting wires.

The remarkable predictions of Gordon Moore in 1965, that the number of transistors per square centimeter on a silicon chip doubles every 18 months [9], has encouraged the constant quest for new technologies that could complement the silicon-based electronics, and molecular electronics is one such technology.

Many decades ago, there were many fundamental questions such as how does the electrical current flow through a single molecule [10, 11]. The concept of electrons passing through a single molecule comes via two different approaches [12]. The first is electron transfer, which involves the charge moving from one end of the molecule to the other. The second one is charge transport, which involves current passing through a single molecule that is connected between electrodes

[13]. The two are closely related because both of them attempt to answer the previous question. From the point of view of fundamental science, molecular electronics could provide an answer for previous inquiry, and perhaps be an ideal way to explore the electronic and thermoelectric conductance through the smallest molecular circuits, where quantum mechanical effects completely dominate [14].

The variety of molecules (both organic and organometallic molecules), together with their various properties could lead to the discovery of new physical phenomena. In addition, molecular junctions could also be promising systems to investigate the basic principles of electron transfer mechanisms. However, there are also other motivations in terms of a technological viewpoint, which is the use of molecules as electronically active elements for many applications. One of these reasons is the size since the typical size of molecules (between 1 and 10 nm) could lead to a higher packing density on a device with subsequent advantages in cost, efficiency and power dissipation [15]. These concepts and many others make molecular electronics an attractive field of science. The desire to make functional molecular devices has pushed the boundaries of measurement and fundamental understanding of a variety of physical phenomena at the single-molecule level, including mechanics, thermoelectrics, optoelectronics, and spintronics, as well as electronic transport [16] as shown in Figure (1.1).

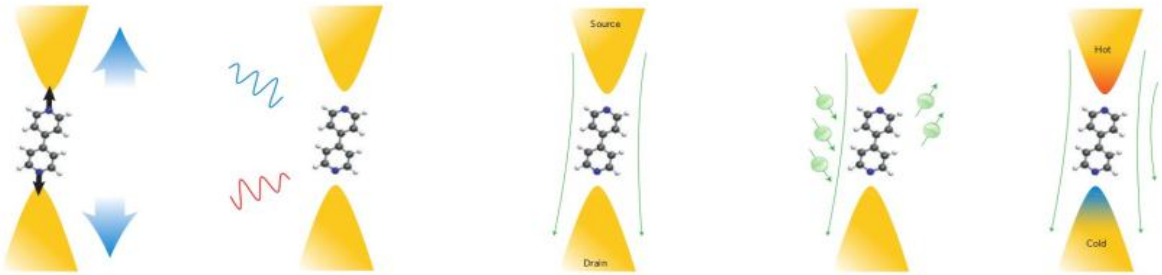

Figure (1.1): Multiple characteristics of single-molecule junctions are being investigated [16].

1.4 Molecular Orbital Theory

Since its inception in the early days of quantum mechanics, the molecular orbital theory has become a powerful method for studying the electronic structure of molecules, illuminating many areas of chemistry. In quantitative form, it has developed both as an ab initio method for computing molecular wave functions directly from the fundamental equations of quantum mechanics and also as a semiempirical technique for interrelating various physical properties of atoms and molecules using a simplified formalism as a framework for parameterization. Until recently, ab initio calculations dealt mainly with very small systems while the semiempirical methods were oriented toward the π electrons of larger planar molecules. In the last few years, however, both approaches have become more concerned with general polyatomic molecules and they now overlap somewhat in their areas of application [17].

The main objective of any theory of molecular structure is to provide some insight into the various physical laws governing the chemical constitution of molecules in terms of the more fundamental universal physical laws governing the motions and interactions of the constituent atomic nuclei and electrons. In principle, such theories can aim at a precise quantitative description of the structure of molecules and their chemical properties, since the underlying physical laws are now well understood in terms of quantum theory based on the Schroedinger equation. However, in practice mathematical and computational complexities make this goal difficult to attain, and one must usually resort to approximate methods [18].

The principal approximate methods considered in molecular quantum mechanics are valence bond theory and molecular orbital theory. The molecular orbital theory has its origins in the early research work in band spectroscopy of diatomic molecules and has been widely used to describe many aspects of

molecular structure and diverse molecular properties such as electronic dipole moments, optical absorption spectra, and electron and nuclear magnetic resonance [17, 19].

Approximate molecular orbital theories are based on schemes developed within the mathematical framework of molecular orbital theory, but with many simplifications introduced in the computational procedure. Often experimental data on atoms and prototype molecular systems are used to estimate values for quantities entering into the calculations as parameters, and for this reason, the procedures are widely known as *semiempirical methods*[19].

1.5 Bonding and Antibonding Molecular Orbitals

The mathematical process of combining atomic orbitals to generate molecular orbitals is called the linear combination of atomic orbitals (LCAO). Quantum mechanics describes molecular orbitals as combinations of atomic orbital wave functions. Combining waves can lead to constructive or destructive interference. In orbitals, the waves can combine with in-phase waves producing regions with a higher probability of electron density and out-of-phase waves producing nodes, or regions of no electron density [20].

Two types of molecular orbitals can from the overlap of two atomic orbitals on adjacent atoms. The in-phase combination produces a lower energy σ_s molecular orbital in which most of the electron density is directly between the nuclei. The out-of-phase addition (or subtracting the wave functions) produces a higher energy σ_s* molecular orbital in which there is a node between the nuclei. The asterisk signifies that the orbital is antibonding. Electrons in a σ_s orbital are attracted by both nuclei at the same time and are more stable (of lower energy) than they would be in the isolated atoms. Adding electrons to these orbitals creates a force that holds the two nuclei together, so these orbitals are called bonding orbitals. Electrons in the σ_s* orbitals are located well away from the region between the two

nuclei. The attractive force between the nuclei and these electrons pulls the two nuclei apart. Hence, these orbitals are called antibonding orbitals. Electrons fill the lower-energy bonding orbital before the higher-energy antibonding orbital [21,22].

In *p* orbitals, the wave function gives rise to two lobes with opposite phases. When orbital lobes of the same phase overlap, constructive wave interference increases the electron density. When regions of opposite phase overlap, the destructive wave interference decreases electron density and creates nodes. When *p* orbitals overlap end to end, they create σ and σ* orbitals. The side-by-side overlap of two *p* orbitals gives rise to a pi (π) bonding molecular orbital and a π* antibonding molecular orbital. Electrons in the π orbital interact with both nuclei and help hold the two atoms together, making it a bonding orbital. For the out-of-phase combination, there are two nodal planes created, one along the internuclear axis and a perpendicular one between the nuclei[22].

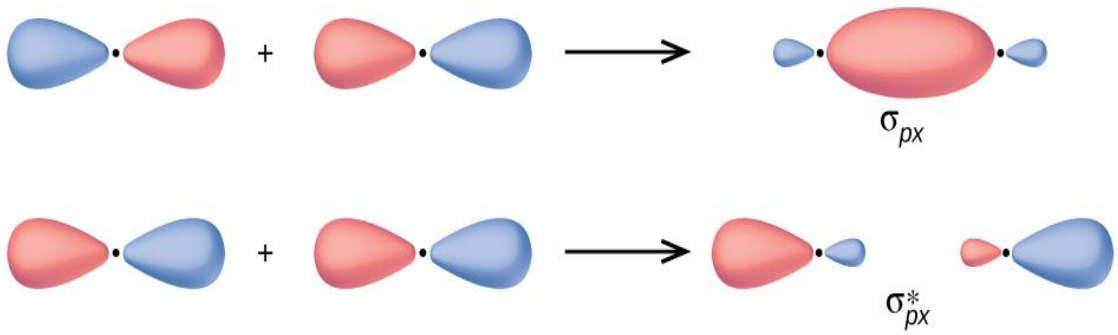

Figure(1.2): Combining wave functions of two *p* atomic orbitals along the internuclear axis creates two molecular orbitals, σ_p and σ^*_p[23].

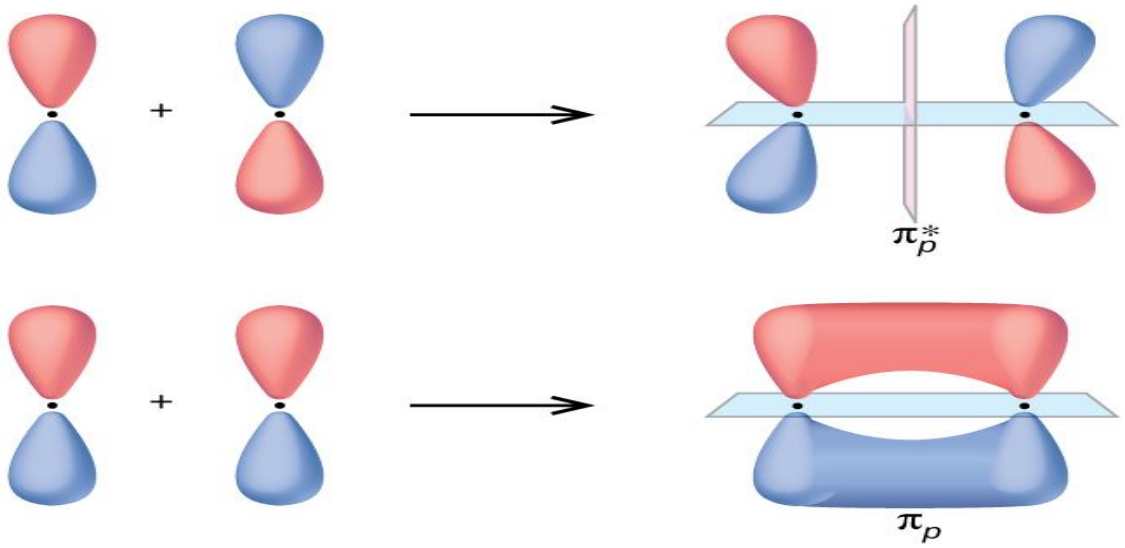

Figure (1.3): Side-by-side overlap of each two *p* orbitals results in the formation of two π molecular orbitals [23].

Combining the out-of-phase orbitals results in an antibonding molecular orbital with two nodes. One contains the internuclear axis, and one is perpendicular to the axis. Combining the in-phase orbitals results in a bonding orbital. There is a node (blue) containing the internuclear axis with the two lobes of the orbital located above and below this node [23].

1.6 Organometallic Material

Organometallic Compounds are chemical compounds that contain at least one bond between a metallic element and a carbon atom belonging to an organic molecule. Even metalloid elements such as silicon, tin, and boron are known to form organometallic compounds which are used in some industrial chemical reactions. The catalysis of reactions wherein the target molecules are polymers or pharmaceuticals can be done with the help of organometallic compounds, increasing the rate of the reactions [24].

Generally, the bond between the metal atom and the carbon belonging to the organic compound is covalent. When metals with relatively high electropositivity (such as sodium and lithium) form these compounds, a carbanionic nature is

exhibited by the carbon which is bound to the central metal atom. An example of an organometallic compound wherein carbons belonging to a benzene molecule bond with chromium is illustrated above. A few more examples of these types of compounds are Grignard reagents, tetracarbonyl nickel, and dimethyl magnesium [25].

1.7 Family of Bipyridine's Molecules

Bipyridines represent the important family of heterocycles, having two pyridines directly linked together giving either symmetrical isomers (2,2′, 3,3′, and 4,4′) or asymmetrical ones (2,3′, 2,4′, and 3,4′) as shown in figure (1.4). These compounds, especially the 2,2' and 4,4' isomers, are known as excellent ligands in coordination chemistry, with an impact in many fields including catalysis and materials chemistry. Besides coordination with metals, the nitrogen atoms of bipyridines can interact with different molecules through non-covalent interactions (hydrogen or halogen bonds), leading to supramolecular structures with interesting properties.

Another important aspect of bipyridine chemistry is the possibility of introducing chirality through ring functionalization or restricted rotation (atropisomers), thus increasing their importance in asymmetry-based applications. Finally, about 4,4'-bipyridines, the quaternization of nitrogens generates viologens, which are known for their good electrochemical properties[27].

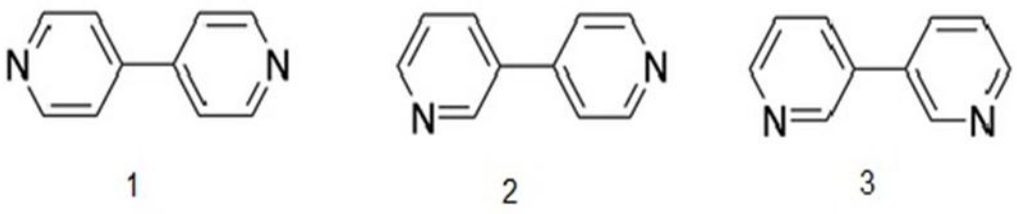

Figure(1.4): The compounds 1, 2 and 3 are the 4,4 bipyridine, 3,4-bipyridine and 3,3-bipyridine respectively[28].

1.8 Historical Review

Zhihai L., 2013 [29], studied the **c**ontrolling charge transport through individual molecules and the effect of anchoring groups on charge transport. Experimental results revealed that the single-molecule conductance values of the porphyrins have followed the sequence of pyridyl > amine > sulfonate > nitrile > carboxylic acid. Electron transport calculations were in agreement that the pyridyl groups result in higher conductance values than the other groups, which was due to a stronger binding interaction of this group to the Au electrodes.

David Zsolt Manrique, *et al*. 2015 [30], investigated the quantum circuit rule for combining quantum interference effects in the conductive properties of oligo(phenylene ethynylene) (OPE)-type molecules possessing three aromatic rings both experimentally and theoretically. The conductances GXmX (GXpX) of molecules of the form X-m-X (X-p-X), with meta (para) connections in the central ring, were predominantly lower (higher), irrespective of the meta, para, or ortho nature of the anchor groups X, demonstrating that conductance was dominated by the nature of quantum interference in the central ring Y. The single-molecule conductances were found to satisfy the quantum circuit rule Gppp/Gpmp/Gmpm/Gmmm.

Oday A. A. Al-Owaedi, 2016 [31], studied the electronic properties of molecules connected to metallic leads, a study included for various families of organic and organometallic molecules, which offer unique concepts and new insights into the electronic properties of molecular junctions, using a combination of density functional theory (DFT) and non-equilibrium Green's function formalism of transport theory.

Qusiy H. Al-Galiby, 2016 [32], presented a series of studies into the electronic and thermoelectric properties of molecular junction single organic molecules: They included perylene Bisimide (PBIs), naphthalene diimide (NDI), Metallo-

porphyrins and a large set of symmetric and asymmetric molecules. Two main techniques included in the theoretical approach, which was Density Functional Theory, which was implemented in the SIESTA code, and Green's function formalism of electron transport, which was implemented in the GOLLUM code.

Mohsin K. Al-Khaykanee 2018 [33], studied the electronic and thermoelectric properties of 12 different organic molecules, using density functional theory DFT, and Green's function formalism, this work included **a** study of the charge transport of 4,4-bipyridine molecules, with a series of sterically-induced twist angles α between the two pyridyl rings. An experiment revealed that the presence of high and low conductance peaks was attributed to different molecule orientations within the junctions. Both experimental measurements using the STM-BJ technique and DFT-based theory reveal that their conductances were proportional to cos2(α), confirming that for both geometries, the electrical current flows through the C-C bond linking the pi systems of the two rings.

Qusiy H. Al-Galiby and Sarah S. Dakh 2019 [34], studied the electronic properties for single-orbital one dimensional, two- dimensional, and diatomic crystalline chains to get a simply qualitative understanding of electronic structure calculation in the periodic systems. The density of states (DOS) is one of the electrical properties that it was used to understand within the band structures that lead to being able to know the mechanism of transport in the materials. The band structure and density of state (DOS) for ordered and disordered systems were performed via a numerical decimation method.

Mohammed N. *et al*.2020 [35], showed that a single pyrene molecule was sandwiched by two copper electrodes in this arrangement. A steady-state theoretical model was used to explore the transport parameters of a single pyrene molecule in four configurations. A gate voltage is generated to the pyrene molecule. Thermoelectric and electron transport features were covered by

combining quantum interaction, contact topology, and gate voltage were all factors to consider. By applying a gate voltage to the pyrene molecule, asymmetric performance and resonance splitting in the transmission spectrum may be achieved properties.

Saisai Y. *et al.* 2021 [36], used the scanning tunneling microscopy break-junction technology, construct and study the conductance and Seebeck coefficient of Anderson-type polyoxometalate (POM) clusters with a single-atom variation. The findings indicated that replacing various center-metal atoms changes the conductance of single clusters by an amplitude and that the electrical conductance of clusters has distinct bias dependence. The central atoms could also affect the Seebeck coefficients of POM clusters.

1.9 The Aims of this Thesis

1-Evaluation of the metal-complexes selectivity in bipyridine molecules and understanding the nature of the metal complexes (Cr, Mo, and W) chemical bond that contacts the complexes to the backbone of the molecule.

2-Investigation of the electronics and optical properties of metal-complexes molecules, which have various central metal atoms to study the effect of the metal-ligand atom on these properties.

3- Using molecules as active elements in nanoscale electronic circuits.

4- Examining of the role of metal-complexes Bipyrimdine molecules on the electrical and thermoelectric transport properties and to design new types of materials, which could offer a route to increasing computing power and optimize thermoelectric materials.

Chapter Two

Theoretical Part

2.1 Introduction

Quantum chemical computations can guide researchers to design and adapt target molecules while lowering the costs connected to experiments, and it is especially beneficial to examine and monitor the High Energy Materials (HEM). Molecular modeling is a set of techniques designed to investigate chemical problems on a computer Computational physicians and chemists can apply one of the following four main methods: Molecular Mechanics (MM), Semi-Empirical (SE), Density Functional Theory (DFT), and Ab initio [37].

Classical mechanics well described Macroscopic systems the exact knowledge of the present state of a classical-mechanical system, one can predict its future state [38].

This principle, however, is not applicable when one dealing with microscopic particles such as electrons or protons. In this case, a quantum mechanical formalism is necessary to describe the state of the microscopic system.

The Heisenberg uncertainty principle demonstrates that the exact momentum and position of a microscopic particle cannot concurrently be determined. So, in order to describe the state of a quantum mechanical system, one need to assume the existence of a function of the particle's coordinates, so called wave function.

To predict the properties of the quantum mechanical system, an equation, describing how the wave function changes with time, is required. For one particle in one-dimensional system, this equation is the Schrödinger equation (Time dependent form) [39].

2.2 Schrödinger Equation for Many Body Systems

Schrödinger equation is the fundamental equation to describe the motions of molecular, atomic and subatomic systems, electrons and nucleus, and even macroscopic systems. The time dependent Schrödinger equation is as the following equation[40,41]:

$$i\hbar\frac{\partial}{\partial t}\Psi(\vec{r},t) = -\frac{\hbar^2}{2m}\nabla^2\Psi(\vec{r},t) + V(\vec{r},t)\Psi(\vec{r},t) = H(\vec{r},t)\Psi(\vec{r},t) \quad \text{.....(2.1)}$$

In simple form:

$$\hat{H}\Psi(\vec{r},t) = E\Psi(\vec{r},t) \quad \text{.....(2.2)}$$

where Ĥ is the energy operator or the Hamiltonian. When the operator Ĥ is independent of time, the Schrödinger equation then reduces to the well-known time-independent equation written for a molecular system[42]:

$$\hat{H}\Psi(\vec{r},R) = E\Psi(\vec{r},R) \quad \text{.....(2.3)}$$

where Ψ(r, R) is the total wave function of the molecular system, r and R are the electron and the nuclei spatial coordinates, respectively, E is the eigen value of the total energy of the system and the total Hamiltonian of the molecular system $\hat{H}$containing M nuclei and N electrons[42,43]:

$$\hat{H} = -\frac{1}{2}\sum_{i=1}^{N}\nabla_i^2 - \sum_{A=1}^{M}\frac{1}{2m_A}\nabla_A^2 - \sum_{i=1}^{N}\sum_{A=1}^{M}\frac{Z_A}{r_{iA}} + \sum_{i=1}^{N}\sum_{j>i}^{N}\frac{1}{r_{ij}} + \sum_{A=1}^{M}\sum_{B>A}^{M}\frac{Z_A Z_B}{r_{AB}}$$

.....(2.4)

In equation (2.4), the total kinetic energy of the molecular system is the sum of the electronic $\hat{T}_e$ and nuclear $\hat{T}_n$ kinetic energies, the total potential energy is the sum of three components, $\hat{V}_{ne}$, the attractive interactions between nuclei and electrons, $\hat{V}_{ee}$, the repulsive electron-electron interactions and $\hat{V}_{nn}$ the repulsive interactions between the nuclei. $Z_{A,B}$ are the nuclei charges of atoms A and B, m_A is the mass of atom A, r_{AB} is the distance between nuclei A and B, r_{iA} is the

distance between nucleus A and electron i, and $\vec{r}_{ij} = |\vec{r}_i - \vec{r}_j|$ is the distance between electrons i and j, ∇_i^2 is the laplacian operator of i electrons.

The electronic and the nuclear motions in molecules in Born-Oppenheimer Approximation, can be separated the total wave function of a molecule takes the form[40,43,44]:

$$\Psi_{total} = \Psi_{electronic} * \Psi_{nuclear} \quad \text{.....(2.5)}$$

The nuclear motion is much slower than the electronic motion because the nucleus is much heavier than the electrons. It could be considered as fixed. The kinetic energy of nuclei is eliminated and the potential energy of nuclei-nuclei could be considered as fixed. So that, the kinetic energy of nuclei and the potential energy of nuclei-nuclei can be eliminated from the Hamiltonian operator, and the Hamiltonian operator $\hat{H}$ is simplified as following[43,44]:

$$\hat{H} = \hat{T}_e + \hat{V}_{Ne} + \hat{V}_{ee} \quad \text{.....(2.6)}$$

The system can actually be described as all electrons moving in a potential field of nuclei with fixed positions.

2.3 Hartree-Fock Methods

The system using the time-independent Schrödinger equation in order to describe the quantum mechanical behavior for all electrons in systems, it is necessary to calculate the many-electron wave functions to solve the Schrödinger equation for all electrons in systems requires solving many of simultaneous differential equations[44,45]. Such a calculation is very difficult and needs simplifying the methods and the problem itself.

Hartree made such a simplification in 1928 through an iterative self-consistent field (SCF) method. Hartree simplified the problem by making an assumption about the form of the many-electron wave functions namely the product of a set of

single-electron wave functions. In a uniform system these wave functions would take the form of simple plane waves. According to the variation principle[49,50], if a given system is described by a set of unknown parameters, the set of parameter values which correctly describes the ground state of the system is just that set of values which minimizes the total energy, this can be expressed as[44,45]:

$$E_{\Phi} = \frac{\langle \Phi | \hat{H} | \Phi \rangle}{\langle \Phi | \Phi \rangle} \geq E_o \qquad \text{.....(2.7)}$$

where E_{Φ} is the lowest-energy eigenvalue of the trial function Φ and E_o is the ground-state energy. Using this theorem, the exact ground-state wave function is approximated from the trial function that gives the lowest energy. Hartree found the Hamiltonian equation of the many-electron system and it was possible to treat each electron separately as a single-particle.

The wave function of Hartree-Fock approach can be written in a compact way as a Slater determinant. The determinant considers the spin of all the electrons and the Pauli exclusion principle. Equation (2.8)below is an example of a Slater determinant for a system of N-electrons [46,47]:

$$\Psi = \frac{1}{\sqrt{N!}} \begin{vmatrix} \Psi_1(1)\alpha(1) & \Psi_1(1)\beta(1) & \Psi_2(1)\alpha(1) & \Psi_2(1)\beta(1) & \dots\dots & \Psi_N(1)\alpha(1) & \Psi_N(1)\beta(1) \\ \Psi_1(2)\alpha(2) & \Psi_1(2)\beta(2) & \Psi_2(2)\alpha(2) & \Psi_2(2)\beta(2) & \dots\dots & \Psi_N(2)\alpha(2) & \Psi_N(2)\beta(2) \\ . & & . & & & . & \\ . & & . & & & . & \\ \Psi_1(N)\alpha(N) & \Psi_1(N)\beta(N) & \Psi_2(N)\alpha(N) & \Psi_2(N)\beta(N) & \dots\dots & \Psi_N(N)\alpha(N) & \Psi_N(N)\beta(N) \end{vmatrix}$$

.....(2.8)

where Ψ is the electronic wave function, α and β are the spin up and spin down of electrons, respectively, and $\frac{1}{\sqrt{N!}}$ is a normalization factor.

The next step in Hartree-Fock methods is to introduce the molecular orbital expansion and determining the corresponding coefficients based on the variation theorem[45]. Solving the Hartree-Fock equation using the iterative process of the self-consistent-field (SCF) producer yields the molecular orbitals ψ (r_i)[44,46].

$$F\Psi_i(\vec{r}) = \varepsilon_i \Psi_i(\vec{r}) \qquad \text{.....(2.9)}$$

For closed shell systems, the Fock operator F takes the form:

$$F = h + \sum_{l=1}^{n/2}(2J_l - K_l) \quad \text{.....(2.10)}$$

where the Coulomb operator J_l and the exchange operator K_l are defined as:

$$J_l\Psi(\vec{r}) = \int \frac{\Psi_l^*(\vec{r})\Psi_l(\overrightarrow{r'})}{\left|\vec{r}-\overrightarrow{r'}\right|} dV'\Psi(\vec{r}) \quad \text{.....(2.11)}$$

$$K_l\Psi(\vec{r}) = \int \frac{\Psi_l^*(\vec{r})\Psi_i(\overrightarrow{r'})}{|\vec{r}-\overrightarrow{r'}|} dV'\Psi(\vec{r}) \quad \text{.....(2.12)}$$

A further restriction involves expanding the molecular orbitals in terms of basis functions φ_i, linear combinations of one-electron functions according to the linear combination atomic orbital (LCAO) method[44,45]. Thus an individual molecular orbital is defined as:

$$\Psi_i = \sum_{\mu=1}^{N} C_{\mu i}\phi_\mu \quad \text{.....(2.13)}$$

$C_{\mu i}$ represents the molecular orbital expansion coefficients. The basis functions φ_i are also chosen to be normalized.

For orbital expansion an appropriate set of basis functions has to be selected, with that the coefficients $C_{\mu i}$ may then be adjusted to minimize the total electronic energy calculated from the many-electron wave function. The resulting value of the energy will then be as close as possible to the exact energy E_o of the ground state of the system within the selected limitations[48].

$$E(\Phi_1, \Phi_2, \dots\dots, \Phi_N) \geq E_o \quad \text{.....(2.14)}$$

The equality sign shall be applied only in case Ψ_i is the exact ground state function.

2.4 Density Functional Theory

Density functional theory (DFT) is a widely quantum mechanical method in physics and chemistry used to investigate the electronic structure of many-electron systems. It is today one of the most important tools for calculating the ground state properties of metals, semiconductors, and insulators. DFT is among the most popular and useful methods available in computational physics and computational chemistry[49].

The starting point of density theory was the Thomas-Fermi model, in 1927, Thomas and Fermi are calculated the energy of an atom by representing its kinetic energy as a function of the electron density, combining this with the classical expressions for the nuclear-electron and electron-electron interactions, which can both also be represented in terms of the electron density[40,43].

The DFT focuses on the much simpler electron density ρ(r). In general, the electron density is the number of electrons N per unit volume for a given state. It is dependent only on three coordinates independently of the number of electrons of the system. Thus[41]:

$$N = \int \rho(\vec{r}) d\vec{r} \qquad \text{.....(2.15)}$$

The central concepts of DFT be dependent on the ground state energy and all other ground state electronic properties are uniquely determined by the electron density. Furthermore, the exact ground state of the system corresponds to the electronic density for minimal total energy.

2.4.1 Hohenberg-Kohn Theorems

Hohenberg and Kohn, in 1964[45] proved that the ground state of a many electron system can be determined by the ground state electron density $\rho(\vec{r})$. The two theorems of Hohenberg and Kohn are[43-48]:

Theorem 1: The ground state energy of a many-electron system is a unique, universal functional of ground state electron density $\rho(\vec{r})$.

Theorem 2: The functional of ground state energy is minimized by the ground state electron density $\rho(\vec{r})$for a many-electron system.

According to above theorems, any ground state properties of a many electron system can be expressed in terms of the ground state electron density $\rho(\vec{r})$. The ground state energy functional $E_V[\rho]$ can be described as[46,50]:

$$E_V[\rho] = \int \rho(\vec{r})\, V_{ext}(\vec{r}) d\vec{r} + F_{HK}[\rho] \qquad \text{.....(2.16)}$$

where $F_{HK}[\rho]$ is a universal functional of $\rho(\vec{r})$to be determined which includes kinetic energy and all the electron-electron interactions, $F_{HK}[\rho]$ is independent of the external potential $V_{ext}(r)$. Considering of the particle conservation, the variation of ground state energy satisfies the following principle[50]:

$$\delta\{E_V[\rho] - \kappa[\int \rho(\vec{r}) d\vec{r} - N]\} = 0 \qquad \text{.....(2.17)}$$

Which gives:

$$\kappa = \frac{\delta E_V[\rho]}{\delta \rho(\vec{r})} = V_{ext}(\vec{r}) + \frac{\delta F_{HK}[\rho]}{\delta \rho(\vec{r})} \qquad \text{.....(2.18)}$$

Where κ is the chemical potential and F_{HK} is a universal functional of electron density. The ground state electron properties of a many-electron system can be obtained exactly from equations (2.17) and (2.18).

Hohenberg-Kohn assumes that F_{HK} exists, but the actual form of F_{HK} is unknown and must be approximated.

2.4.2 Kohn-Sham Equations

Depending on Hoherberg-Kohn theorems, the energy functional $F_{HK[\rho]}$ of an interacting many-electron system can be expressed as[51]:

$$F_{HK}[\rho] = T[\rho] + \frac{1}{2}\iint \frac{\rho(\vec{r})\rho(\overrightarrow{r'})}{|\vec{r}-\overrightarrow{r'}|} d\vec{r}d\overrightarrow{r'} + E_{xc}[\rho] \quad \text{.....(2.19)}$$

Where T[ρ] is the kinetic energy of a system, the second term is the classical Coulomb energy and the third term $E_{xc}[\rho]$ is the exchange-correlation energy which describes the non-classical interaction of electrons including all the many-body effects. Because the concrete expression of functional T[ρ] and $E_{xc}[\rho]$ were not given, one could not carry out a first principle calculation. In order to solve this problem, Kohn and Sham assuming that, a non-interacting many-electron system which has the same electron number N and ground state electron density $\rho(\vec{r})$ under an external potential $V_{ext}(\vec{r})$ with those of an interacting many-electron system[46]. The Kohn-Sham assumption is: for a non-interacting system, $\rho(\vec{r})$ can be expressed by a set of ancillary orthogonal functions $\psi_i(\vec{r})$ as:

$$\rho(\vec{r}) = \sum_i \psi_i^*(\vec{r})\psi_i(\vec{r}) \quad \text{.....(2.20)}$$

with $\langle \psi^i | \psi^j \rangle = \delta_{ij}$.

The Kohn-Sham kinetic energy is given by:

$$T_{KS}[\rho] = -\frac{\hbar^2}{2m}\int \sum_{i=1}^{N} \psi_i^*(\vec{r})\nabla^2\psi_i(\vec{r})d\vec{r} \quad \text{.....(2.21)}$$

Considering the many-body interaction, the true kinetic energy T[ρ] in equation (2.19) is not equal to $T_{KS}[\rho]$. The difference between them can be combined with exchange-correlation functional $E_{xc}[\rho]$ as[46-49]:

$$E_{xc}[\rho] = T[\rho] - T_{KS}[\rho] \quad \text{.....(2.22)}$$

and the ground state energy functional can be written as:

$$E_V[\rho] = T_{KS}[\rho] + \frac{1}{2}\iint \frac{\rho(\vec{r})\rho(\overrightarrow{r'})}{|\vec{r}-\overrightarrow{r'}|} d\vec{r}d\overrightarrow{r'} + E_{xc}[\rho] + \int d\vec{r}\,\rho(\vec{r})V_{ext}(\vec{r}) \quad \text{.....(2.23)}$$

By applying the variation principle to equation (2.23):

$$\frac{\delta}{\delta\psi_i^*(\vec{r})}\{E[\rho] - \int d\vec{r}\sum_i \varepsilon_i\psi_i^*(\vec{r})\psi_i(\vec{r})\} = 0 \qquad \text{.....(2.24)}$$

This leads to the Kohn-Sham equations:

$$\left\{-\frac{\hbar^2}{2m}\nabla^2 + \int \frac{\rho(\overrightarrow{r'})}{|\vec{r}-\overrightarrow{r'}|}d\overrightarrow{r'} + V_{XC}[\rho] + V_{ext}(\vec{r})\right\}\psi_i(\vec{r}) = \varepsilon_i\psi_i(\vec{r}) \qquad \text{.....(2.25)}$$

Where $V_{XC}[\rho]$ is the exchange-correlation potential which has been modified to include all the difference between the interacting and non-interacting kinetic energy in equation (2.22), $V_{XC}[\rho]$ takes the form:

$$V_{XC}[\rho] = \frac{\delta E_{XC}[\rho]}{\delta\rho(\vec{r})} \qquad \text{.....(2.26)}$$

We should note that the Kohn-Sham equation has to be calculated self-consistently considering that the wave function $\psi_i(r)$ is influenced by the electron density $\rho(\vec{r})$ which is included in Hamiltonian. Through solving a set of Kohn-Sham equations (2.25) self-consistently, one can obtain the total energy of the system:

$$E = \sum_i^N f_i\varepsilon_i - \frac{1}{2}\iint \frac{\rho(\vec{r})\rho(\overrightarrow{r'})}{|\vec{r}-\overrightarrow{r'}|}d\vec{r}d\overrightarrow{r'} + E_{XC}[\rho] - \int d\vec{r}\,\rho(\vec{r})V_{ext}(\vec{r}) \qquad \text{.....(2.27)}$$

The physics of Kohn-Sham equation is unlike to that of Schrödinger equation. The significance of Kohn-Sham equations consists in that it reduced an interacting many-body problem to a set of independent equations which describes the state of single electron in the effective potential of other electrons [50].

The major problem of DFT is to find the exchange-correlation energy E_{XC}, used so far as a mathematical term. This term includes all the effects of exchange and correlation interactions, such as Pauli exclusion between electrons with same spin orientations, and the instantaneous reaction of electrons with opposite spins. If the exact exchange-correlation function is known, the system is solved exactly. As previously noted, this function is from the difference of the Hamiltonian between

the interacting many-electron systems to the non-interacting single electron system[40].

2.4.3 The Local (Spin) Density Approximation (L(S)DA)

The local density approximation (LDA) is the simplest approximation to $E_{\times c}[\rho(\vec{r})]$, which assumes the system is a homogenous electron gas and $E_{\times c}[\rho(\vec{r})]$ depends only on the local value of electron density. Therefore, $E_{\times c}[\rho(\vec{r})]$ can be written in a simple form[42,44]:

$$E_{XC}^{LDA}[\rho] = \int \rho(\vec{r})\, \varepsilon_{XC}\big(\rho(\vec{r})\big) d\vec{r} \qquad \text{.....(2.28)}$$

Compared to LDA, the local spin density approximation LSDA defines the exchange correlation potential in terms of the density of α and β spins and was developed for calculating the properties of open-shell systems[44].

$$E_{XC}^{LSDA}\big[\rho_\alpha, \rho_\beta\big] = \int \rho(\vec{r}) \varepsilon_{XC}\big(\rho(\vec{r})_\alpha, \rho(\vec{r})_\beta\big) d\vec{r} \qquad \text{.....(2.29)}$$

Where ε_{XC} is the exchange correlation energy per particle.The LSD approximation provides better results than HF for certain properties such as equilibrium structures, vibrational frequencies and dipole moments.

In general, the LSDA provides reliable information for those systems that closely resemble a uniform electron gas, namely those in which the density varies slowly with position. However, in reality, atomic and molecular systems do not possess uniform electron densities and thus more sophisticated models are required[47].

2.4.4 The Generalized Gradient Approximation (GGA)

The electron density in a real molecule varies greatly from position to position. To get a more accurate approximation of the exchange-correlation energy, functional which include not only the electron density, but also the gradient of the electron density were developed[40,42].

$$E_{XC}^{GGA}\big[\rho_\alpha, \rho_\beta\big] = \int f\big(\rho_\alpha, \rho_\beta, \nabla\rho_\alpha, \nabla\rho_\beta\big) d\vec{r} \qquad \text{.....(2.30)}$$

This functional generally offer an improvement over the LSDA since they account for the variation of density with position. To simplify the problem, E_{XC} is often written as the sum of an exchange (E_X) and correlation (E_C) terms[45]:

$$E_{XC} = E_X + E_C \quad \text{.....(2.31)}$$

The exchange-energy functional can then be obtained from the HF exchange term with the Kohn-Sham orbitals in place of the HF orbitals, and approximate solutions for E_C are sought. Various exchange and correlation functional have been developed independently and can be combined in various ways. For instance, one popular GGA functional is BLYP, where Becke's 1988 exchange functional is paired with the Lee-Yang-Parr correlation functional[40].

2.4.5 The Hybrid Functional

The hybrid exchange-correlation functional is widely used functional, it combine the exchange-correlation GGA functional and an exact exchange functional, ultimately yielding a method that is somewhere between HF and GGA. The most popular hybrid functional, B3LYP, uses Becke's 1988 exchange functional E_X^{B88} and Lee, Yang and Parr's correlation functional E_C^{LYP} as gradient corrections to the LSDA exchange and correlation functional[42, 51].

$$E_{XC}^{B3LYP} = (1-a)E_X^{LSDA} + aE_{XC}^{HF} + bE_X^{B88} + cE_C^{LYP} + (1-c)E_C^{LSDA} \text{...(2.32)}$$

Here, the three parameters, a specified the amount of exact exchange (a =0.20), b and c control the contribution of exchange and correlation (b=0.72 and c=0.81)[55].

2.5 Basis Sets

A basis set is a set of functions used to describe the shape of the orbitals in an atom. Molecular orbitals and entire wave functions are created by taking linear combinations of basis functions and angular functions. Most Semiempirical methods use a predefined basis set. When ab initio or density functional theory calculations are done, a basis set must be specified. Although it is possible to create a basis set from scratch, most calculations are done using existing basis sets. The type of calculation performed and basis set chosen are the two biggest factors in determining the accuracy of results[40,43].

2.5.1 Slater Type Orbitals (STO's)

Slater type functions are exponential that mimic the exact eigen functions of the hydrogen atom. A typical STO is expressed as[40,43]:

$$\chi^{STO} = Nr^{n-1}e^{-\xi r}Y_{lm}(\theta,\varphi) \quad \text{..... (2.33)}$$

Where N is a constant of normalization, n is a principal quantum number and ξ is a constant related to the effective charge of the nucleus. Y_{lm} is a spherical harmonics which describes the angular part of the wave function. Slater type functions show a correct behavior nears the nuclei at r → 0 with a discontinuous behavior.

2.5.2 Gaussian Type Orbitals (GTO's)

Gaussian type orbitals (GTOs) can be written in terms of Cartesian coordinates as[44,45]:

$$\chi^{GTO} = Nx^{l_x}y^{l_y}z^{l_z}e^{-\xi r^2} \quad \text{..... (2.34)}$$

N is a normalization factor. The sum of angular momentum lx, ly and lz determines the type of orbitals. ξ Represents the orbital exponent that shows how compact (large ξ) or diffuse (small ξ) is the resulting function. The r^2 dependence

in the exponential is a deficiency of the GTOs with respect to the Slater-type orbitals STOs[48,53].

GTOs have two main problems. First an improper behavior nears the nuclei at $r \rightarrow 0$, second problem is that GTO falls off too rapidly far from the nuclei compared with the STO. Therefore, the tail of the wave function in the GTO is represented poorly.

A rough estimate says that three times as many GTOs as STOs are required in order to reach the same level of accuracy. One of the disadvantages of STOs is that many-center integrals such as Coulomb and HF-exchange terms are difficult to compute with STOs. Therefore, it does not play a role in modern wave function based quantum chemistry codes. One of the advantages of the Gaussian basis set is that the product of two Gaussian functions is another Gaussian function. As a result, for the calculations of Coulomb and HF-exchange terms the analytical solution is available for the Gaussian functions. Therefore the GTO basis function in HF and related methods is popular because very efficient algorithms exist for analytically calculating the many-center integrals[54,49].

In order to improve the GTO basis sets, one usually employs a contracted GTO basis set, in which several primitive Gaussian functions are mixed to give a contracted Gaussian function (CGF) as[43]:

$$\chi_j^{CGF} = \sum_i^M C_{ij}\chi_a^{GTO} \qquad \text{.....(2.35)}$$

Here, M is the number of Gaussian primitives used in a linear combination. The basis sets used in Gaussian are classified into minimal basis sets, split valence sets, polarization and diffuse functions and others[43].

2.5.2.1 Minimal Basis Sets

The minimal basis set is the minimum number of basis functions χ needed to describe the ground states of the component atoms in a molecule. A common name of minimal basis sets is STO-nG, the n (n=2 to 6) represents the number of Gaussian primitive functions that comprise a single basis function[48]. In these basis sets, the same number of Gaussian primitives comprises core and valence orbitals. Minimal basis sets typically give rough results that are insufficient for research-quality publication, but are much cheaper than their larger counterparts. The following are examples of commonly used minimal basis sets: STO-2G, STO-3G, STO-6G [40,43].

2.6.2.2 Split-Valence Basis Sets

The inner-shell atomic orbitals in terms of a split-valence basis set are represented by one basis function and the valence orbitals are represented by two or more basis functions[55]. One easy method to extend a basis set is to increase the number of basis functions used per orbital. Split-valence basis sets employ more than one basis function of variable orbital exponents for each valence orbital and only one basis function for each core orbital. For instance, the valence double-zeta (VDZ) basis set uses two basis functions per valence orbital while the valence triple-zeta (VTZ) uses three, and so on. While the split valence basis sets provide a better description of the molecular orbitals because they allow for variable atomic size, they still are not able to provide a balanced basis set on their own[56].

2.5.2.3 Polarization and Diffuse Functions

Polarization functions are functions of higher angular momentum such as d- and f- type functions for heavy atoms and p- and d-type functions for hydrogen and helium atoms[57,58]. This increases the flexibility of the basis set by allowing the

shape of the orbital to change (i.e., become polarized in one direction). The inclusion of polarization functions can be important for systems in which hydrogen is involved such as hydrogen-bonding and proton transfers since these will allow the s orbital to become distorted from its regular spherical shape. Polarization functions are used because they often result in more accurate computed geometries and vibrational frequencies[40,58]. The addition of polarization functions in terms of the Pople basis set nomenclature is indicated in brackets after the contraction scheme while diffuse functions denoted by '+'. For instance, the 6-31++G(d, p) basis set includes a set of d-type functions on all heavy atoms and p-type functions on hydrogen and helium. The first '+' indicates that diffuse s- and p-type functions are included on heavy atoms, while the second '+' indicates that diffuse s-type functions have been included on hydrogen. Another group of basis sets that are often used are those of Dunning and co-workers. These are the correlation-consistent polarized valence (double/triple/…etc)zeta basis sets, cc-pVXZ, where X indicates the degree of splitting. These were developed specifically for use in calculations that include electron correlation[59,60]. For heavy metals, the relativistic Effective-Core Potentials (ECPs) such as Stuttgart Dresden triple zeta ECPs (SDD) basis set is used. The types of Los Alamos Nationwide Laboratory 2-double-zeta (LANL2DZ) and SDD basis sets are powerfully recommended for heavy metals. Scalar relativistic corrections are more rigorous than ECPs and spin-free computes are not much more expensive[42].

2.6 Computed Properties

2.6.1 HOMO, LUMO and Energy Gap

The two most important molecular orbitals MOs are called the frontier orbitals in which they lie at the outmost boundaries of the electrons of the molecules, these MOs are the highest occupied molecular orbital HOMO and the lowest unoccupied molecular orbital LUMO. The band gap is the difference of the energies between the two orbitals HOMO and LUMO[61,62].

$$E_{gap} = E_{LUMO} - E_{HOMO} \quad \text{.....(2.36)}$$

The energy gap helps not only to control the way the molecule interacts with other species, but also to describe the chemical reactivity and the stability of the molecule. A molecule with a small band gap is generally associated with a high chemical reactivity, low stability and soft molecule[63]. When an electron transfer to a higher energy state filling unoccupied molecular orbitals, and is call the excited state from the ground state [64,65]. At the HF Level, Koopmans theorem suggest that the energy of the HOMO is a good approximation to the negative experimental ionization potential (-IP) [62]. Similarly, he suggests that the electron affinity (EA) for an N- electron system is equal to the negative of the LUMO energy, assuming that the orbitals do not relax [64].

In general, the prediction of the EA using KT is unreliable due to the generally large effect of orbital relaxation on the LUMO eigenvalue. In addition to the question of the effect of relaxation on the validity of KT, there has been a substantial uncertainty as to the degree of physical significance of the KS orbitals of DFT applied within the KS framework [66,67].

2.6.2 Fermi Energy

The fundamental variation principle in DFT is the Fermi energy. Fermi energy used to measure the escaping trend of a cloud of electrons. It is a constant through all space, and can be calculated due to the following equation [68]:

$$E_F = \left[\frac{\partial E}{\partial N}\right] v_{(\vec{r})} \quad \text{…….. (2.37)}$$

Where E is the energy and N is the number of electrons.

Experimentally, Fermi energy is related to IP and EA, as in the following equation [69,70]:

$$E_F \approx \frac{1}{2}(E_{HOMO} + E_{LUMO}) \approx -\frac{1}{2}(IP + EA) \quad \text{……..(2.38)}$$

2.6.3 Electrochemical Hardness

The hardness in H is a measurement of molecule resistance to the change or deformation. defined as [71]:

$$H = \frac{1}{2}\left[\frac{\partial \mu}{\partial N}\right]_{V(\vec{r})} \quad \text{…….(2.39)}$$

The hardness is central of the energy gap between HOMO and LUMO, molecule has large energy gap called hard molecule. In terms of IE and EA, the hardness is calculated as [72, 73]:

$$H = \frac{(IE - EA)}{2} \quad \text{……(2.40)}$$

In DFT, the electrochemical hardness is the second derivative of electronic energy with respect to the number of electrons N, for a constant external potential V(r) [73].

$$H = \frac{1}{2}\left[\frac{\partial^2 E}{\partial N^2}\right]_{V(\vec{r})} \quad \text{……..(2. 41)}$$

2.6.4 Electronic Softness

The electronic softness of a molecule is associated with the energy gap that the molecule has, soft molecule has a small energy gap, its electron density change more easily than a hard molecule. A small energy gap means small excitation energies to the manifold of excited states, therefore, soft molecules will be more reactive than hard molecules [73]. The electronic softness is calculated according to the relationship [62]:

$$S = \frac{1}{2H} = \left(\frac{\partial^2 N}{\partial E^2}\right)_{V(r)} = \left(\frac{\partial N}{\partial \mu}\right)_{V(r)} \quad \text{.....(2.42)}$$

2.6.5 Electrophilicity index

Electrophilicity index is a measure of energy lowering due to maximal electron flow between donor and acceptor. Electrophilicity index (ω) is defined as [74]:

$$\omega = \mu^2 / 2H \quad \text{.....(2.43)}$$

Where μ is the electronic chemical potential, the electrophilicity is built up from the electronic structure of molecules, independent of the nucleophilic. The electrophiles are species that stabilize upon receiving on additional amount of electronic charge from the environment [75].

2.6.6 Electrical Conductance

Electrical conductance is an simplicity expression of which an electric current flows through a material. When a current of one Ampere passes through a component across which a voltage of one Volt exists, then the electrical conductance of the component is one Siemens(S)[76, 77]:

$$G = I/\mathrm{v} \quad \text{.....(2.44)}$$

The electrical conductance *G* was computed from the Landauer formela:

$$G = G_0 \int_{-\infty}^{\infty} dE\, T(E) \left(-\frac{df(E)}{dE}\right) \quad \text{.....(2.45)}$$

Where $f(\mathrm{E})$ is the Fermi function:

$$f(\mathrm{E}) = [e^{\beta(E-E_F^{DFT})} + 1]^{-1} \quad \text{.....(2.46)}$$

E_F is the Fermi energy and $\beta=1/k_BT$,

G_0 in equation (2.45) is the quantum of conductance:

$$G_0 = \left(\frac{2e^2}{h}\right) \quad \text{.....(2.47)}$$

Since the quantity $(-\frac{df(E)}{dE})$ is a probability distribution at $E=E_F$, with a width of order k_BT [78,79].

2.6.7 Seebeck Coefficient

Seebeck coefficient is a measure of a magnitude of an induced thermoelectric voltage in response to a temperature difference across a material. Seebeck coefficient is also defined thermoelectric power and thermoelectric sensitivity of a material, it is measured in volts per kelvin (V/K) in SI units. Seebeck coefficient of a material is calculated from equation (2.48) when a small temperature gradient is applied to a material as[45]:

$$S = -\frac{\Delta V}{\Delta T} \quad \text{..... (2.48)}$$

Where ΔT is a small temperature difference between the two ends of a material and ΔV is the thermoelectric voltage seen at the ends.

2.6.8 Transmission Coefficient

If the wave propagation is considered in a discontinues medium, then the transmission coefficient is describe the amplitude and intensity of a transmitted wave comparative to an incident wave[80]. The transmission coefficient and the associated reflection coefficient in non-relativistic quantum mechanics are used to describe the waves incident behavior on a barrier, the transmission coefficient is used to refer to the probability of tunneling of a particle through a barrier. The probability flux of the transmitted wave comparative to that of the incident wave is represented in terms of transmission coefficient [81,82]. The transmission coefficient of the structure was placed between two electrodes. The transmission coefficient *T(E)* describes the propagation of electrons of energy *E* from one electrode to the other. *T(E)* was calculated by finding the Hamiltonian *H* and the matrices of overlap *S* [83].

2.6.9 Current–Voltage (I–V)

(I-V)characteristics are widely measured experimentally, so a routine to calculate I-V curve is useful for characterizing the new structures. The current (I), with respect to voltage (V), can be calculated from the transmission probability [81]:

$$I(V) = \frac{2e}{h} \int_{E_f - \frac{eV}{2}}^{E_f + \frac{eV}{2}} T(E,V)\, dE \qquad \text{.....(2-49)}$$

In this equation: (e) electronic charge, (h) blank constant, T(E) transmission coefficient, the transmission depends on the bias voltage. For small voltages, however, the current can be approximated by using the zero-bias transmission probability[81]:

$$I(V) = \frac{2e}{h} \int_{E_f - \frac{eV}{2}}^{E_f + \frac{eV}{2}} T(E,0)\, dE \qquad \text{.....(2-50)}$$

For a perfectly periodic system, the transmission probability $T(E)$ is equal to the number of open channels at energy (E).

2.6.10 Figure of Merit

A figure of merit of electron (ZT_e) is a quantity used to characterize the performance of a device, system or method, relative to its alternatives. In engineering, figures of merit are often defined for particular materials or devices in order to determine their relative utility for an application. In analytical calibration, they are employed to compare the relative performances of different analytical methodologies, and also to establish detection capabilities, a feature which is specific for analytical chemistry.The figure of merit (ZT_e) is computed from the formula [82,83]:

$$(ZT_e) = S^2GT/k_e \qquad \text{..... (2.46)}$$

Where S is the Seebeck coefficient (thermopower), G is the electrical Conductance, T is the absolute temperature, and k_e is the thermoelectric Conductance. In order to maximize ZT_e, it is clear that both the thermopower and electrical conductance have to be high while the thermoelectricl Conductance must be low.

2.7 The Software

All calculations in this study have been performed by using the Gaussian 09 package of programs, Gauss View 5.0.8, Gauss Sum 3.0, SIESTA and GOLLUM Programs. These programs are described as below:

2.7.1 Gaussian 09

Gaussian is a very high- end quantum chemical software package, available commercially through Gaussian, Inc. The Software run on virtually all computer platforms, including Microsoft Windows. In addition, it can be, accessed through Web based, interface tools such as Web MO. Gaussian is the most powerful software available to, educators and student researchers through the North Carolina School Computational, Chemistry server.The "09" refers to the year 2009 in which the software was published. G09 is most recent version [84].

Gaussian, a commercial quantum chemical software package from Gaussian, Inc., considered by many (including the authors of this resource) to be the industry standard in the area of molecular modeling and computational, chemistry. Gaussian is capable of running all of the major methods in molecular modeling, including molecular, mechanics: ab initio: semi- empirical: and density functional theory (DFT).

It is probably best known for its robustness in running ab initio and DFT calculations. Gaussian also does several compound methods such as MPx and Gx, where x is a number that indicates the level of the method. For example, there is MP2 and MP4, defined as, Moller-plesset 2nd order and moller- plesset 4th order. The name Gaussian comes from the use of the Gaussian Type Orbital's that Gaussian's originator, John Pople, used to try to overcome the computational difficulties that arose from the use of Slater Type Orbital's. Most readers will know

the Gaussian mathematics by two other names – a normal distribution, or perhaps as a *bell- shaped curve*. A number of researchers, such as S.F. Boys and Isaiah Shavitt, Pople, quite brilliantly, recognized that the (relatively) simple, substitution of a series of Gaussian functions for the Slater function, would greatly simplify the rest of the calculation of the Schrödinger, equation. Pople's work resulted in the standard use of these Gaussian functions. Virtually every other developer of ab initio computational, chemistry software uses this technique. Pople, by the way, was awarded the 1998 Nobel Prize in Chemistry (along with Walter Kohn, who you will hear about later) for this work [85].

2.7.2 Gaussian View 5.0.8 Program

Gaussian is the most powerful software available to, educators and student researchers through the North Carolina School Computational, Chemistry server. Gauss view program is designed to import the input files for the Gaussian programs and also used to demonstrate the output files for Gaussian program in the dimensional photo, Gaussian view which is not used as calculation program, but it facilitates the work on Gaussian program and supply the users with three major advantages. Enable the user to draw the molecules including the big one, also enables the rotation, transferring and changing it size easily by the mouse. The complex input preparation for the routine work and the advanced method. Finally Gaussian view permit the inspection of Gaussian calculations results using variety of geometrical technique's and this involve to balanced molecular patterns, molecular orbits and electronic density surfaces.

Gaussian is capable of running all of the major methods in molecular modeling, including molecular, mechanics: ab initio semi-empirical and density functional theory (DFT). The name Gaussian comes from the use of the Gaussian

Type Orbital's that Gaussian's originator, John Pople, used to try to overcome the computational difficulties that arose from the use of Slater Type Orbital's [86].

2.7.3 Gauss Sum 3.0

The Gauss Sum 3.0 is a software application recorded by Noel O'Boyle. Gauss Sum 3.0 uses the plotting program (Gnuplot17) for picture graphs. The Gauss Sum is that can examines the output of widely computational physics and chemistry program (such as Gaussian 09 program)[87].

Gauss Sum can get ready more information such as a geometry optimization, plot the density of states (DOS) spectrum, source information on the UV-Vis. Transition states, scheme the UV-Vis spectrum and the circular dichroism spectrum, abstract data on IR and Raman vibrations and plotting the IR and Raman spectra, which may be scaled using general or individual scaling.

Throughout the computational studies carried out in this study, Gauss Sum 3.0 has been used in the ground state calculation of DFT to plotting the IR, Raman and DOS spectra. Also for the excitation state calculation of TD-DFT it is used to plotting the UV-Vis spectrum and it is showed the excitation energies, electronic transition configurations and oscillator strengths for the optical transitions for the studied nanocomposites[88].

2.7.4 SIESTA Program

SIESTA (Spanish Initiative for Electronic Simulations with Thousands of Atoms) is both a method and its computer program implementation, to perform efficient electronic structure calculations and ab initio molecular dynamics simulations of molecules and solids. SIESTA's efficiency stems from the use of strictly localized basis sets and from the implementation of linear-scaling algorithms which can be applied to suitable systems. SIESTA is main characteristics are use the standard Kohn-Sham self-consistent density functional

method in the Local Density Approximations and ..(LDA-GGA). It uses norm-conserving pseudo potentials in their fully nonlocal (Klein man-Bylander) form. It uses atomic orbitals as a basis set, allowing unlimited multiple-zeta and angular momenta, polarization and on site orbitals. Finite-support basis sets are the key for calculating the Hamiltonian and overlap matrices in the operations. Projects the electron wave functions and density onto a real-space grid in order to calculate the Hartree and exchange-correlation potentials and their matrix elements. Finally, Besides the standard Rayleigh-Ritz eigenstate method, it allows the use of localized linear combinations of the occupied orbitals (valence-bond or Wannier-like functions), making the computer time and memory scale linearly with the number of atoms. Simulations with several hundred atoms are feasible with modest workstations. It routinely provides total and partial energies, atomic forces, stress tensor, electric dipole moment, electron density, geometry relaxation, constant-temperature molecular dynamics, variable cell dynamics, k-sampling of the Brillion zone, local and orbital-projected DOS, vibrations (phonons), band structure and ballistic electron transport [89].

In a system that has a large number of atoms containing complex potentials there is large computational expense for time and memory. One method to solve the computational problem is to reduce the number of electrons by introducing the pseudopotential approximation which was proposed by Fermi in 1934. This method, has developed from creating non-relativistic empirical pseudopotentials to more realistic ab-initio pseudopotentials. The idea of this concept that the electrons in an atom are split into two parts, the first is core and the second is valence, where core electrons lie within filled atomic shells as well as they are spatially localized around the nucleus. Whereas, the valence electrons are arranged in partially filled shells, and they are the ones contributing to the formation of molecular orbitals. Therefore, this reduces the number of the electrons in a system considerably.

Moreover, in the SIESTA code a special kind of ab-initio pseudopotential which called the norm-conserving pseudopotential [33] is carried out.

2.7.5 GOLLUM Program

Gollum is a program that computes the charge, spin and thermal transport properties of electrical junctions having an arbitrary number of leads[90]. The program needs to read as inputs the junction arrangement as well as its corresponding Hamiltonian in order to generate those transport properties. Gollum reads model tight-binding Hamiltonians as well as Hamiltonians generated using density functional theory programs. It is based on the non-equilibrium Green's function (NEGF) formalism for one particle Hamiltonian. In its present form it uses density functional theory with the numerical implementation contained in the code (SIESTA)[91] However, Gollum computational scheme is very general and can be implemented together with any electronic structure methods based on localized basis sets. A good knowledge of SIESTA and the SIESTA's input files is necessary since only the Gollum commands are described in although a complete input file.

Chapter Three

Results and Discussions

3.1 Electronics Properties

3.1.1 Introduction

To investigate the electronics properties of the family's meta-complexes bipyrimdine, many researchers have been studying pyridine and its many derivatives to develop and produce a variety of metal complexes of interest. Therefore, the aim behind choosing those molecules and their complexes with transition metal were their interesting structures and spectroscopic properties, which is one of the most appealing topics in coordination chemistry and material science [92].

The metal-complexes characteristics of the family of molecules that were involved bipyridine (1), bipyrimdine (2), and X(CO)4-bipyrimdine (3) molecules with metal complexes and CO group were studied using Density-Functional Theory and Time-Dependent (DFT/TD-DFT). A striking feature of the metal complexes that have been used as a result of presenting values of bandgap energy (LUMO-HOMO) and displaying subtly different electronic characteristics. These compounds were been chosen to present a further examination of the behavior of metal complexes and to appear the influence of supporting metal ligands in molecular junctions. Furthermore, LUMO and HOMO are the lowest unoccupied molecular orbitals and the highest occupied molecular orbitals, respectively. In addition, to give more accurate details about the properties of these molecular structures.

This chapter presents the computational method and results of structural and electronic properties of bipyridine, bipyrimdine, and X(CO)4-bipyrimdine-molecules. The Gaussian 09 package implements the DFT, which is a good and dependable theory [93]. The Lee-Yang– Parr gradient-corrected correlation potential (B3LYP) and the "Becker's three-parameter gradient-corrected exchange potential" were used, and all calculations were performed by using the 6-311G

as a basis set, and for metal complexes structures (Cr, Mo, and W) were used the LANL2DZ basis set for that, which were determined to be accurate for the systems that contain metal complexes.

In the present study, the steps of the work consisted of three stages: firstly, molecules were been optimized to get the preferred configurations. Secondly, the vibrational properties were calculated, and finally, the time-dependent Schrödinger equation was used to calculate the UV-Visible spectrum calculations and the possibility of optical applications. DFT/TD-DFT at the B3LYP was used to calculate the electronics properties by Gaussian 09 program.

3.1.2 Geometrical Optimization

The technique of attempting to discover the molecule's minimal energy arrangement is known as topology optimization. The technique calculates the wave function and energy for a certain starting geometry before moving on to a new geometry with lower energy. This process is continued until the geometry with the lowest energy is discovered. The method determines the force on each atom by calculating the gradient of the energy concerning atomic locations.

At each stage, advanced algorithms were employed to select a new geometry, to achieve quick convergence to the geometry with the lowest energy. It is significant to note that this approach will not always lead to the global minimum or the geometry with the least amount of energy.

At the B3LYP/6-311G and (LANL2DZ) levels of the theory, the molecular geometries investigated in this work were optimized in the ground state.

Figure (3.1a) and Figure (3.1b) show the molecular geometries that optimization calculations will run on it, those bipyridine, Bipyrimdine, and X(CO)4-bipyrimdine molecules. In our work, the main aim is to evaluate the metal-complexes selectivity in bipyridine molecules and understand the nature of

the metal complexes (Cr, Mo, and W) chemical bond that contacts the complexes to the backbone of the molecule.

Bipyridine

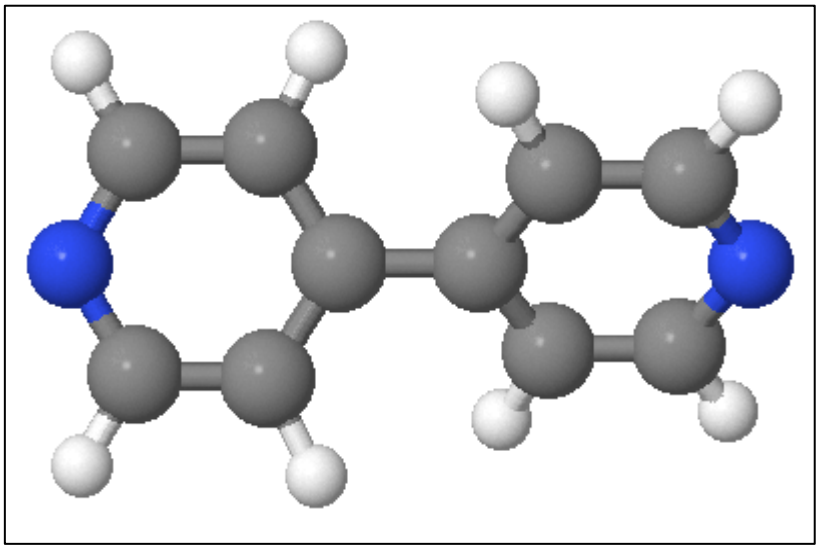

Bipyrimdine

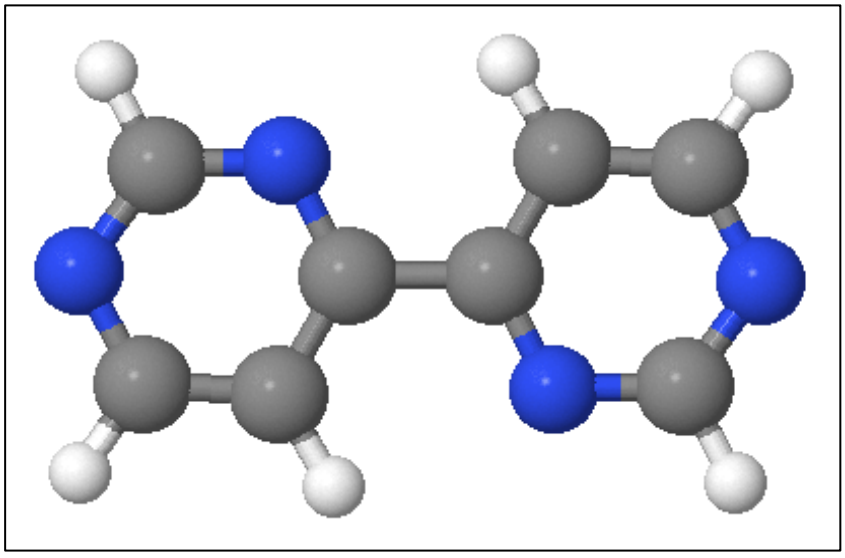

Figure (3.1 a): The Optimized Geometric Structures of Studied Molecules Bipyridine and Bipyrimdine (grey: carbon, white: hydrogen, blue: nitrogen, red: oxygen).

X(CO)4-bipyrimdine

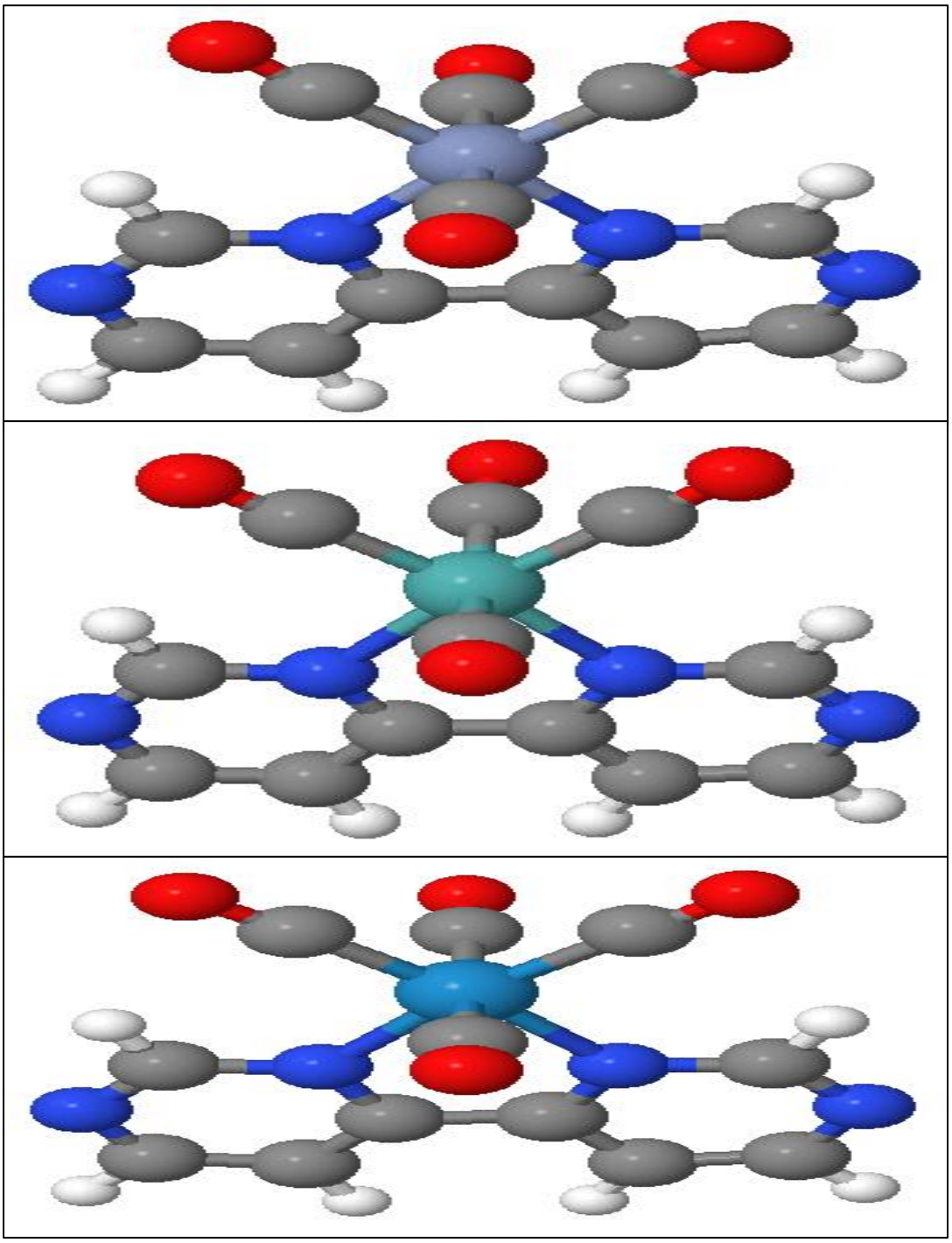

Figure (3.1 b): The Optimized Geometric Structures of Studied Molecules of X(CO)4-Bipyrimdine Molecules.
(grey: carbon, white: hydrogen, blue: nitrogen, red: oxygen, green: X = Cr, Mo, W).

After performing the geometry optimization process, the following tables were obtained that show the values of the bond length and the angles. Tables (3.1)-(3.5) show the optimized geometric parameters for studied molecules (bond lengths in Angstrom, and dihedral angles in degree calculated by B3LYP/6-311G method.

Table (3.1): The optimized geometric parameters (lengths in Angstrom and angles in degree) of Bipyridine.

Bond Length (Å)		**Dihedral angle (deg)**	
Bond	**Value**	**Bond**	**Value**
N1=C1	1.34	D(N1=C1-C3=C5)	0.0
C1-H1	1.1	D(N1-C2=C4-C5)	0.0
C1-C3	1.4	D(C3=C5-C6-C8)	40.0
C3-H3	1.1	D(C3=C5-C6=C7)	-140.0
C2=C5	1.41	D(C4-C5-C6=C7)	40.0
C5-C4	1.41	D(N2=C9-C7=C6)	0.0
C4=C2	1.399	D(N1-C10=C8-C6)	0.0
N1-C2	1.34		
C5-C6	1.487		
C6=C7	1.41		
C7-H5	1.1		
C7-C9	1.399		
C9-H7	1.1		
C9=N2	1.34		
N2-C10	1.34		
C10-H8	1.1		
C10=C8	1.4		
C8-H6	1.1		
C6-C8	1.41		

Table (3.2): The optimized geometric parameters (lengths in Angstrom and angles in degree) of Bipyrimdine.

Bond Length (Å)		**Dihedral angle (deg)**	
Bond	**Value**	**Bond**	**Value**
N1-C1	1.342	D(N1-C1=C3-C4)	0.1
C1-H1	1.1	D(N1=C2-N2=C4)	0.1
C1=C3	1.4	D(C3-C4-C5-N3)	-0.1
C3-H3	1.1	D(N2=C4-C5=C6)	-0.1
C3-C4	1.4	D(C3-C4-C5=C6)	180
C4=N2	1.345	D(C5-N3=C7-N4)	-0.1
N2-C2	1.337	D(C5=C6-C8=N4)	-0.1
C2=N1	1.34		
C4-C5	1.482		
C5-C6	1.4		
C6-H4	1.1		
C6-C8	1.399		
C8-H6	1.1		
C8=N4	1.342		
N4-C7	1.341		
C7-H5	1.1		
C7=N3	1.336		
C5-N3	1.345		

Table (3.3): The optimized geometric parameters (lengths in Angstrom and angles in degree) of Cr(CO)4-Bipyrimdine.

Bond Length (Å)		**Dihedral angle (deg)**	
Bond	**Value**	**Bond**	**Value**
N1-C1	1.342	D(N1-C1=C3-C5)	0.3
C1-H1	1.1	D(N1=C2-N2-C5)	0.6
C1=C3	1.4	D(N2=C5-C8=N3)	2.7
C3-H3	1.1	D(C8=N3-C11=N4)	0.6
C3-C5	1.4	D(C8-C10=C12-N4)	0.2
C5-N2	1.345	D(N2=C5-C8-C10)	-176.8
N2-C2	1.337		
C2=N1	1.34		
N2-Cr	2.0658		
C5-C8	1.459		
O2-C6	1.16		
C6-Cr	1.906		
Cr-C7	1.907		
Cr-N3	2.068		
Cr-C9	1.865		
C7-O3	1.16		
C8-N3	1.367		
C8-C10	1.4		
C10-H4	1.1		
C11-N3	1.36		
C9-O4	1.16		
C10-12	1.4		
C11-H5	1.1		
C11-N4	1.323		
C12-N4	1.346		

Table (3.4): The optimized geometric parameters (lengths in Angstrom and angles in degree) of Mo(CO)4-Bipyrimdine.

Bond Length (Å)		**Dihedral angle (deg)**	
Bond	**Value**	**Bond**	**Value**
N1-C1	1.342	D(N1-C1=C3-C5)	-0.1
C1-H1	1.1	D(N1=C2-N2-C5)	0.0
C1=C3	1.384	D(N2=C5-C8=N3)	0.6
C3-H3	1.1	D(C8=N3-C11=N4)	0.2
C3-C5	1.397	D(C8-C10=C12-N4)	0.1
C5-N2	1.364	D(N2=C5-C8-C10)	-179.1
N2-C2	1.354		
C2-H2	1.1		
C2=N1	1.318		
N2-Mo	2.225		
C5-C8	1.454		
O2-C6	1.156		
C6-Mo	2.053		
Mo-C7	2.053		
Mo-N3	2.229		
Mo-C9	1.984		
C7-O3	1.155		
C8-N3	1.363		
C8-C10	1.397		
C10-H4	1.1		
C11-N3	1.355		
C9-O4	1.16		
C10-C12	1.385		
C11-H5	1.1		
C11-N4	1.317		
C12-N4	1.342		
C12-H6	1.1		

Table (3.5): The optimized geometric parameters (lengths in Angstrom and angles in degree) of Bipyrim W(CO)4-Bipyrimdine.

Bond Length (Å)		**Dihedral angle (deg)**	
Bond	**Value**	**Bond**	**Value**
N1-C1	1.348	D(N1-C1=C4-C5)	-0.4
C1-H1	1.1	D(N1=C2-N2-C5)	-0.1
C1=C4	1.393	D(N2=C5-C8=N3)	-7.1
C3-H3	1.1	D(C8=N3-C11=N4)	-0.9
C4-C5	1.405	D(C8-C10=C12-N4)	-0.5
C5-N2	1.367	D(N2=C5-C8-C10)	171.2
N2-C2	1.359		
C2-H2	1.1		
C2=N1	1.321		
N2-W	2.242		
C5-C8	1.464		
O2-C3	1.166		
C3-W	2.022		
W-C7	2.076		
W-N3	2.254		
W-C9	2.022		
C7-O3	1.160		
C8-N3	1.368		
C8-C10	1.405		
C10-H4	1.1		
C11-N3	1.355		
C9-O4	1.16		
C10-C12	1.393		
C11-H5	1.1		
C11-N4	1.322		
C12-N4	1.348		
C12-H6	1.1		

It is obvious from Tables (3.1)-(3.5) that the geometrical parameters calculations by the present method are in good agreement with experimental data [94]. The difference of atomic numbers for the conjugated atoms affects the bond length between these atoms and these Tables declare that the convergence between the bonds C-C and C-N comes from the convergence between their atomic numbers, and this reason explains the difference of the C-H bond.

The N-X Bond Length between metal-nitrogen bands and central metal complexes in bipyrimdine molecules as shown above Table in which these data were measured after optimizing all molecules at ground state that were used in this work by using Gaussian 09 program as mentioned above.

3.1.3 Molecular Orbitals and Energy Gap

Table (3.6) shows the high occupied molecular orbital energy E_{HOMO}, lower unoccupied molecular orbital energy E_{LUMO}, and energy gap E_g for Bipyridine, Bipyrmidine, Cr(CO)4-Bipyrim, Mo(CO)4-Bipyrim, and W(CO)4-Bipyrim molecules.

Table (3.6): E_{HOMO}, E_{LUMO} and energy gap E_g Bipyridine, Bipyrmidine, Cr(CO)4-Bipyrim, Mo(CO)4-Bipyrim, and W(CO)4-Bipyrim molecules.

Complexes	**HOMO (eV)**	**LUMO (eV)**	**E_g (eV)**
Bipyridine	-0.26080	-0.07107	0.18973
Bipyrmidine	-0.26549	-0.09895	0.16654
Cr(CO)4-Bipyrim	-0.19908	-0.12811	0.07097
Mo(CO)4-Bipyrim	-0.21480	-0.13984	0.07496
W(CO)4-Bipyrim	-0.21399	-0.14209	0.0719

From Table (3.6) which illustrates the calculated values of E_{HOMO}, E_{LUMO} and energy gap (E_{gap}) in eV for the family of metal-complexes (X(CO)4) with bipyrimdine molecules, it had been clear that the energy gap value various for those molecules, in particular after attaching the metal complexes with CO group, this energy gap values reduce compared to bpy and bpyrim molecules. This is due to many reasonable cases: 1- pi-conjugated system[95], that is considerably appeared the charge transport through the linked bond. 2- Metal complexes give distinctive properties of these compounds, which helped in reducing the energy gap due to the conduction property of metals complexes, they are conductive materials.

3.1.4 Molecular Orbital Charge Distribution

Figure (3.2) shows plots of the HOMOs and LUMOs. As predicted from previous studies, the HOMOs and LUMOs were stretched throughout the backbone for each molecule in this diagram. This figure illustrates charge density localization and delocalization patterns of these frontier molecular orbitals (FMOs). Furthermore, it had been predicted to appear a special behavior in particular after adding metal complexes to these molecules to appear more importantly results as shows in FMOs energy. In addition, FMOs energies present that weight of density of states focused the most case on the metal groups (X(CO)4) as shown in the HOMOs energies, whereas it can be seen the density distribution of the charge in other parts of the molecule was less much than metal complexes. This gives great importance to these metal complexes that had been used in this work to give an advantage in the multiple uses with such types of organic molecules. Therefore, tetra carbonyl derivatives that we have used in this study were strongly colored may be to an intense Cr, Mo, and W metal-ligand charge transfer.

Figure (3.2) shows the charge distribution in those molecules, and to know the role of metal complexes at different types. Therefore, it has been exhibed through the figures the mechanism of distributing charges on the parts of the molecules, in particular with metal complexes.

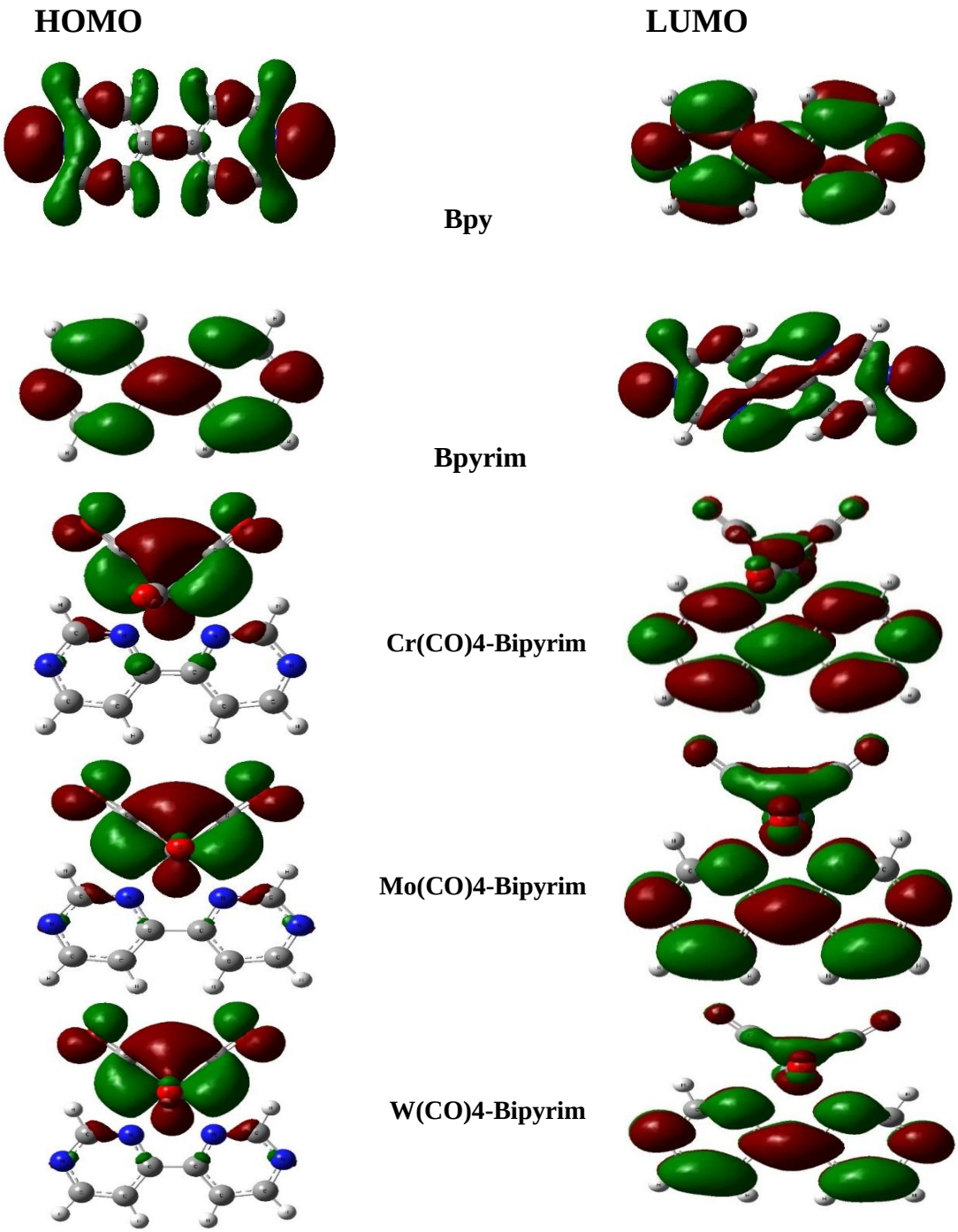

Figure (3.2): Distribution pattern of the important FMOs of molecules 1–5 at B3LYP/6-311G (LANL2DZ) level of theory.

3.1.5 IR Spectroscopy Analysis

The IR spectra of these molecules were presented in Figure(3-3a) which is evident that bpy and bpyrim molecules show the peaks of absorbance, which display three peaks at 1624 cm^{-1}, 1561 cm^{-1}, and 833 cm^{-1} that were attributed to bpy molecule. As well as the peaks at 1589 cm^{-1} and 1547 cm^{-1} that be attributed to bpyrim molecule. The difference and the shifting in those peaks for bpy and bpyrim that occurs may be due to the chemical structures and the pi-conjugated system between two rings shown in Figure(3.3a) after replacing carbon atoms with nitrogen atoms on both sides of pyridine rings.

In addition, for metal complexes with bipyrim, the changeable behavior of the peaks had been seen, in particular, Mo(CO)4 and W(CO)4 was exhibited their peaks were identical in most of the values of these metals such as at bands 1883 cm^{-1} and 1967 cm^{-1}. However, in the case of Cr(CO)4 displays two overlapping strong peaks at 2310 cm^{-1} and 2380 cm^{-1} were appeared different behavior because of the bandgap value and the length bond N-Cr in both sides of phenyl rings. Thus, upon the normal and complexation cases, the ligand undergoes structural changes, which affect the values of absorbance for these molecules as shown in Figure(3.3b).

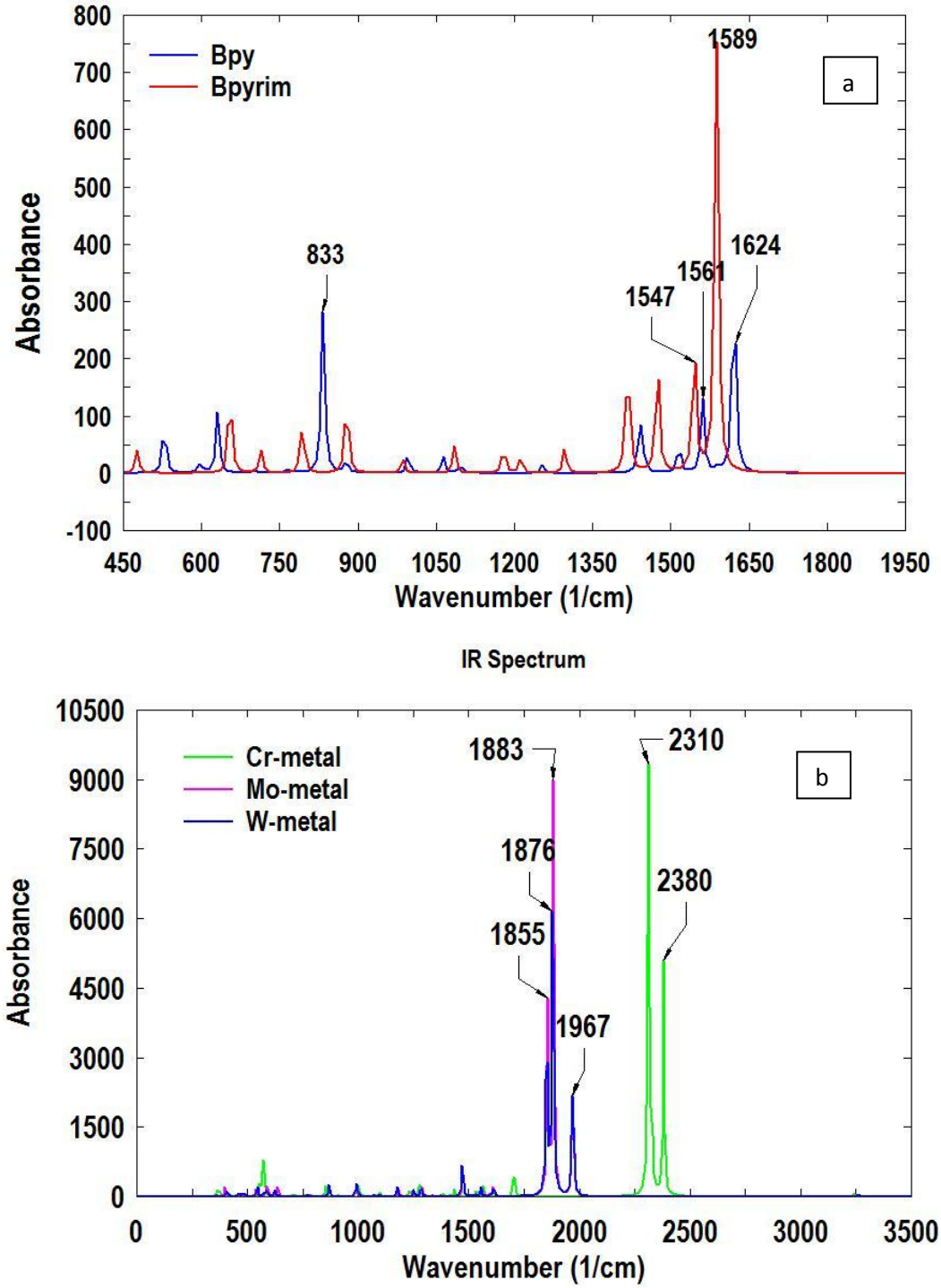

Figure (3.3): IR spectra of (a) bpy (black), bpyrim(green), and (b) X(CO)4 with bpyrim molecules showing a shift and stretch of the peaks for the studied molecules.

The spectrum resulting from IR Analysis was explained by using some lists as shown in Figure (3.4) [96].

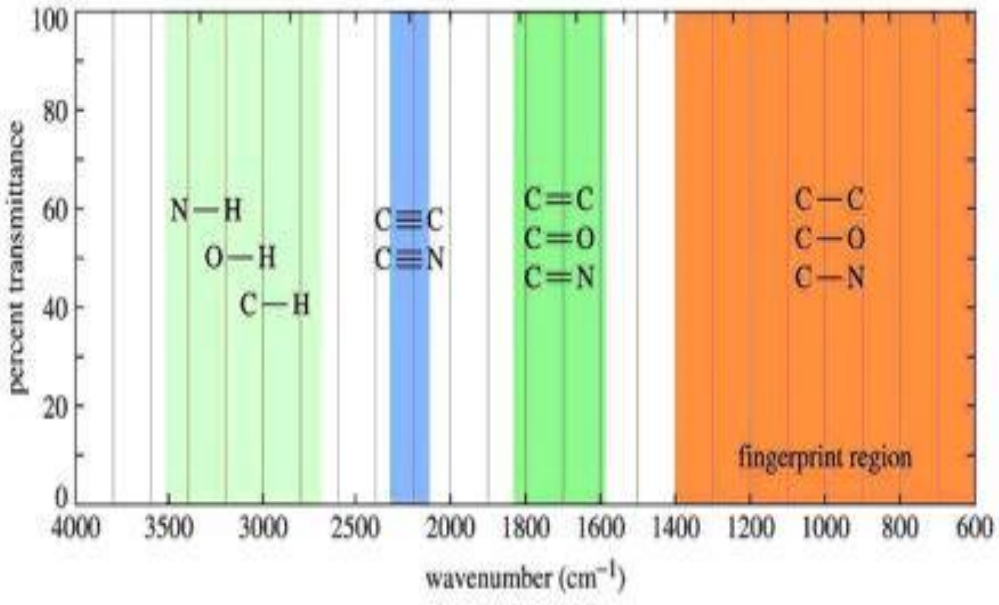

Figure (3.4): The IR spectroscopy frequency ranges, the appearance of the vibration, and absorptions for functional groups[101].

3.1.6 Ultraviolet-Visible (UV-Vis) Spectroscopy

The UV-vis spectrum has been calculated for bipyridine, bipyrimdine, and X(CO)4-bipyrimdine molecules as shown in Figure(3.5). It had been seen the range of wavelength for five molecular structures is involved visible light, which is 296 (black) nm, 359 (green) nm, 652(blue) nm, 658(red) nm, and 744(pink) nm, respectively. The change of designed structure of bpy and bpyrim was a considerable role to shift the range of wavelength from 296 nm to 359 nm this is due to the pi-conjugated system between two pyridine rings [97]. Furthermore, the torsion angles of bpy and bpyrim is 40^{o} and 0^{o}, which means that the effect of the pi-conjugated system in bpy was more than bpyrim due to the overlap and interaction between the two rings. However, the metal complexes play a more important to shift the range of UV light from 359 nm to 652-658 nm for W(CO)4 and Mo(CO)4 with bipyrimdine, respectively.

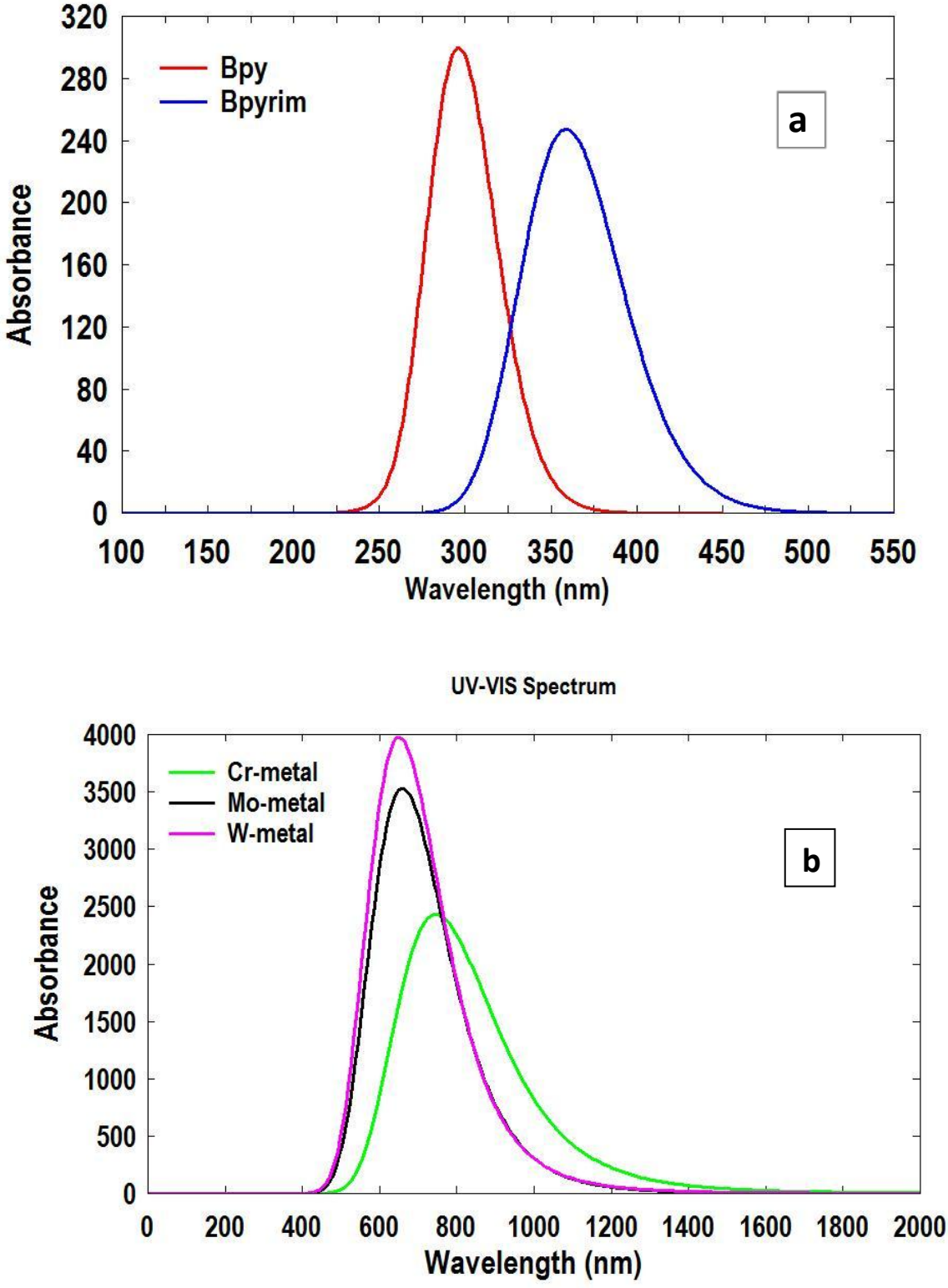

Figure (3.5): The UV-Visible spectra for (a) bipyridine, bipyrimdine, and (b) X(CO)4 bipyrimdine molecules.

3.1.7 Density of State (DOS)

Figure (3.6) represents the density of states (DOS) of the bipyridine, bipyrimdine, and bipyridine metal complex compounds. In all compounds, the degeneracy of occupied molecular orbitals is larger than that of the virtual molecular orbitals.

The DOS was distributed in the occupied orbitals greater than in the virtual orbitals, this behavior is since the energies of LUMO are greater than that for HOMO energies. For bipyridine metal complex compounds, the electron can easily transform from the occupied orbitals to virtual orbitals in comparison with the others, because the DOS in the occupied orbitals are more than DOS in the virtual orbitals. This behavior makes these compounds behave suitable for electronic applications when interacting with other species and play an important role in electron transfer.

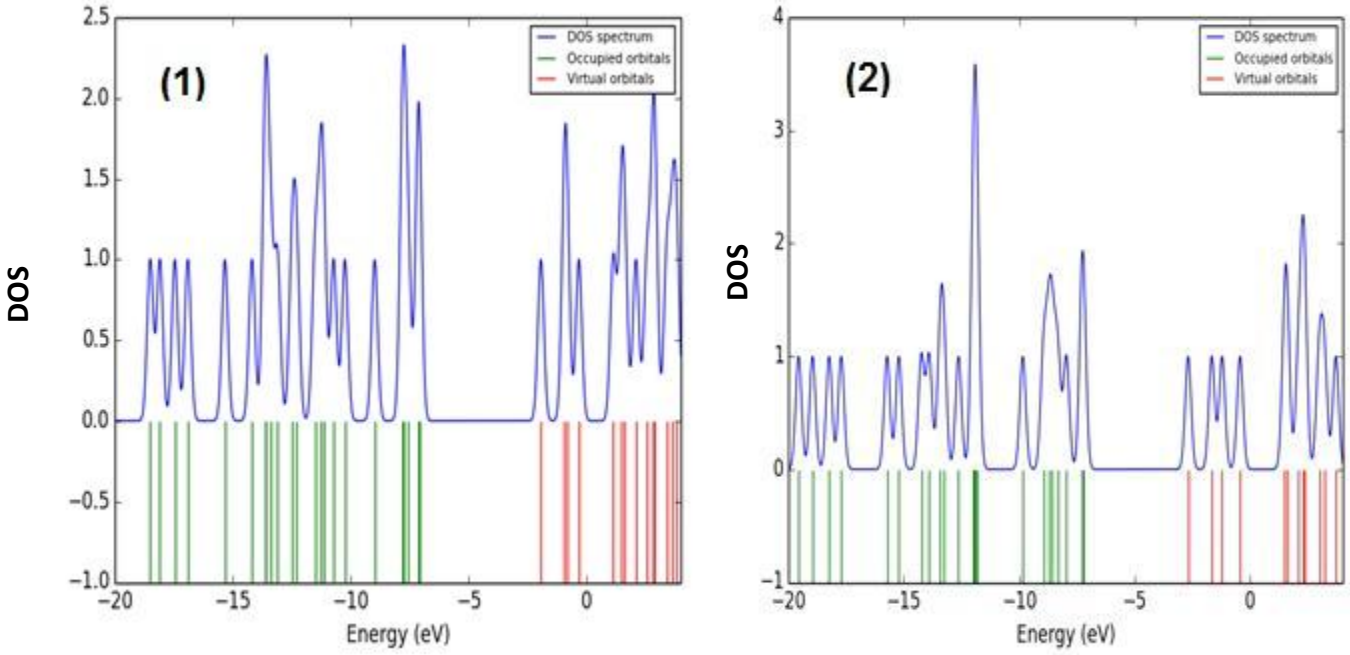

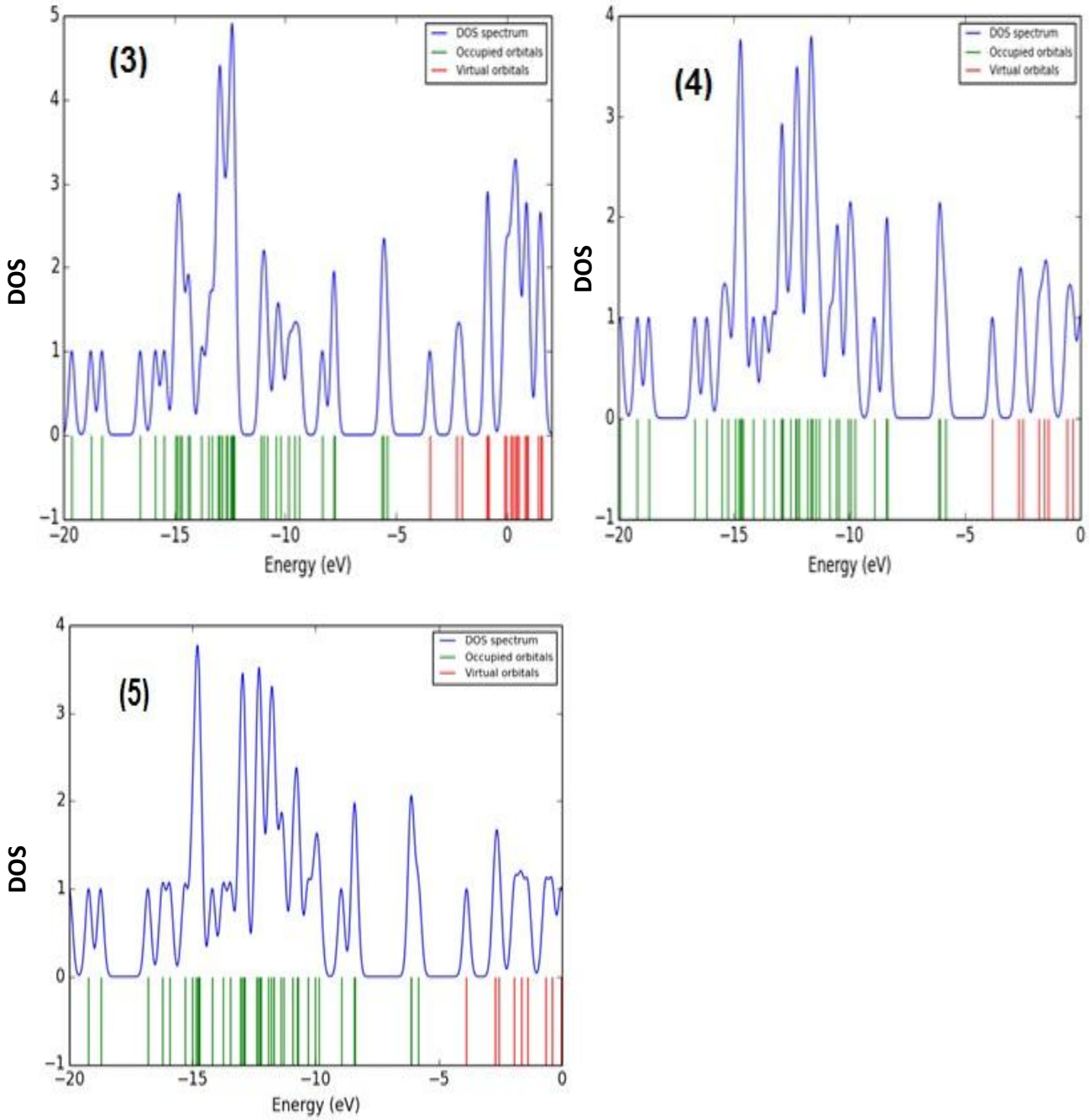

Figure (3.6): The Density of State for (1) bipyridine, (2) bipyrimdine, and (3,4,5) X(CO)4 bipyrimdine molecules.

3.1.8 Some Electronic Properties of the Studied Structures

Some parameters were computed, and they are called Reactivity parameters Indices. They refer to the activity of the members of a series of compounds and their derivatives compared to each other. These parameters can be calculated from the energy of the Frontier Molecular Orbitals (HOMO and LUMO).

These variables can be computed at the optimal shape of the molecule. The top of the orbital is occupied by electrons HOMO, its negative energy will be greater than the lowest orbital that is empty or unfilled with electrons LUMO, and the three most important and most widespread parameters have been known in scientific references as follows[98]:

The Hardness (H) is a measure of the difficulty or hardness in giving electrons, which indicates chemical stability. It is worth noting that the reciprocal of the hardness is referred to as the ductility in giving up electrons, and this scale is called Softness = 1/2H the fluidity scale.

Chemical potential (μ), it is a measure of the ability to reactivity. The low energy of LUMO measures the electrophilicity, i.e. the ability to gain electrons, and the high value of HOMO energy measures the ability to give electrons. Electrophilicity (ω), a measure of the willingness to find or attract electrons[98].

It is clear from the numerical values that Cr(CO)4-Bipyrimdine is the most chemically reactive compound, as it has the lowest electronic hardness of these compounds (the lowest value of the modulus H).

Whereas, it shows the highest ability to exchange electrons (the highest value of the models μ), while the compounds appear W(CO)4-Bipyrimdine the highest desire to gain more electrons (the highest numerical value of the coefficient ω).

Table:3.7 contains results obtained from simple were calculated for (1) bipyridine, (2) bipyrimdine, and (3,4,5) X(CO)4 bipyrimdine molecules.

Structures	**$\mu = (E_{LUMO} + E_{HOMO})/2$**	**$H = (E_{LUMO} - E_{HOMO})/2$**	**$\omega = \mu^2/2H$**
Bipyridine	-0.16593	0.094865	0.14511
Bipyrmidine	-0.18222	0.08327	0.19937
Cr(CO)4-Bipyrimdine	-0.16359	0.035485	0.377060
Mo(CO)4-Bipyrimdine	-0.17732	0.03748	0.41942
W(CO)4-Bipyrimdine	-0.17804	0.03595	0.44086

3.2 The Thermoelectric Properties

3.2.1 Introduction

Electrical transport through organometallic molecular junctions that have attracted wide attention for specific electronic operations as an alternative to silicon-based technologieunder arising ever-increasing challenges facing miniaturization of electronic devices, which has seen a renaissance in the field of molecular electronics over ten years[99-101]. In addition, electrical properties through metal-molecule-metal junctions depend on the chemical structures of the single-molecules that are difficult to in such a molecular type of devices[102]. Advances in single-molecule devices have driven a wealth of knowledgeable scientific-related development the electronic and thermoelectric properties of such systems, as well as the mechanisms that are used to transport the charge through it [103-105]. The field of molecular electronics has gotten a lot of interest as researchers look into nanoscale thermoelectricity in the hopes of developing new organic thermoelectric materials that are more environmentally sustainable [106, 107].

In this section, the Bipyridine (Bpy) and metal-complexes bipyrimdine (Bpyrim) molecules were studied due to intensely observes their wavelengths in the visible part of the spectrum. Therefore, the electron and thermoelectric transport are attributed to metal-ligand charge transport. As well as these components of molecular electronics and metal complexes were having electrochemically switchable characteristics are of interest [108, 109].

3.2.2 Computational Method

To calculate the electrical and thermoelectric properties of the molecular structures under study, the relaxed molecules were found by using DFT/ SIESATA software [110]. DFT-based SIESTA code was carried out to get completely optimized structures of the gas phase molecules. In addition, it has been used a double-zeta polarized (DZP) which is the basis set for all molecules, and also the generalized gradient approximation (GGA) for the exchange and correlation functional[111, 112].

In addition, on a real-space grid formed by a plane-wave cutoff of 250 Ry, the Hamiltonian and overlap matrices were computed. The transmission coefficient of electrons passing through the molecule from the left lead to the right lead is then calculated by using GOLLUM code [101]. The electrical calacution were carried out at Lancaster University, United Kandim.

3.2.3 Geometry of Studied Molecules

To study the electrical and thermoelectric properties for set molecular structures, and after relaxing all isolated molecules, they were attached through two gold leads as shown in Figure(3.7). As in the experimental results the angle of bipyridine molecule approximates between the two rings to be around was 34^{o} [103-105]. In our DFT calculations, the torsion angle was found about 40^{o}. However, the torsion angle of bipyrimdine molecule is 0^{o} due to the overlap between the pi-orbitals which increases when the rings are rotated perpendicular to each other as shown in Table (3.8), and the electrical transport follows a $\cos^{2}\theta$ [106]. For X(CO)4-bipyrimdine molecules, the angle between the two rings was found 0^{o} because a metal linked atom (W, Mo, and W) via two pyridine rings in those structures.

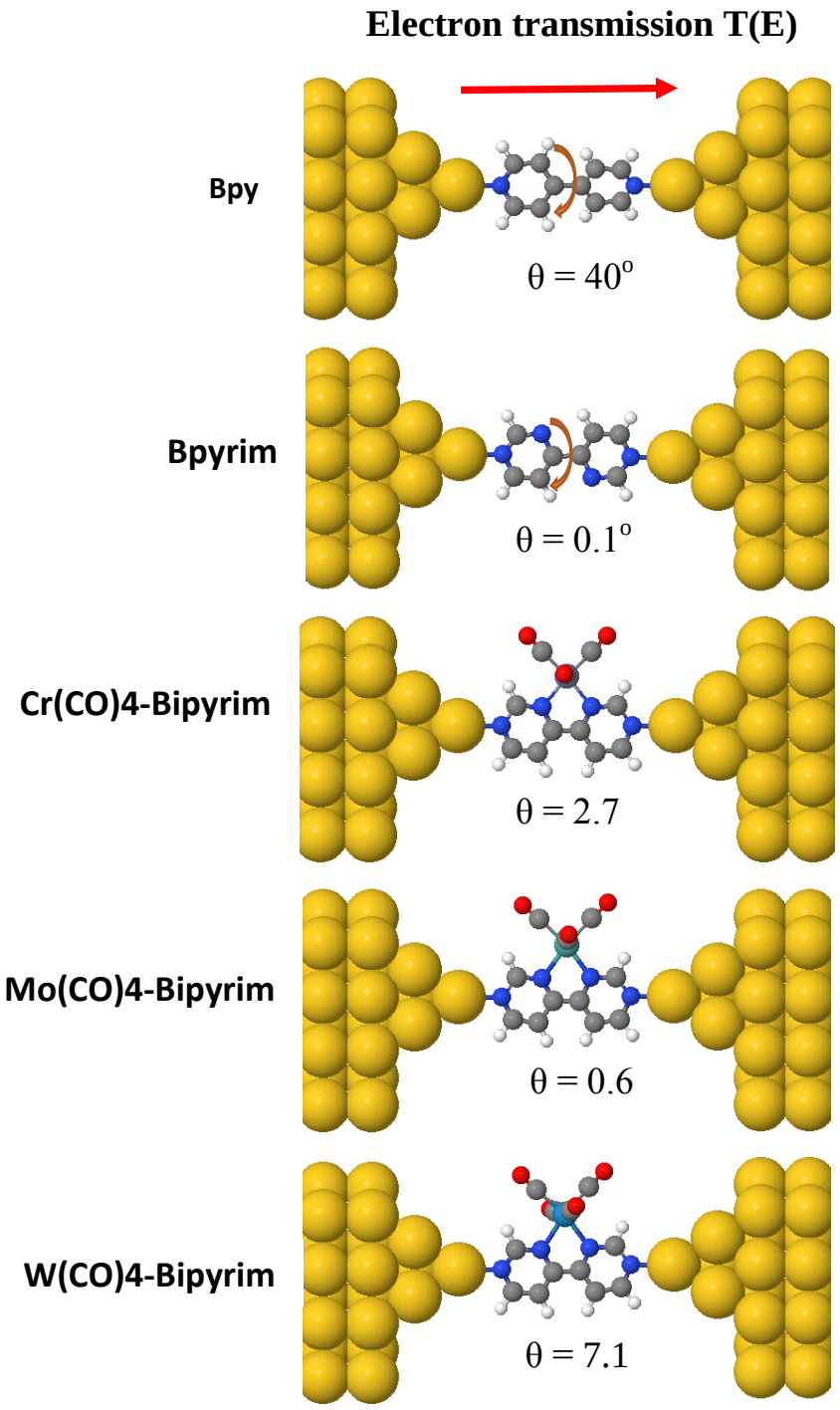

Figure (3.7): Molecular structures of a set of Bpy, Bpyrim, and X(CO)4-Bipyrimdine molecules between two gold leads at different metal centre (Cr, Mo, W) complexes.

Table(3.8): The molecular structures with the dihedral angle between two pyridel rings as experiment. and theoretical data.

Molecule	Dihedral angle/ exp.	Dihedral angle/ theo.
Bpy	34^{o} [107]	40^{o}
Bpyrim	-	0.1^{o}
Cr-metal-bpyrim	-	2.7^{o}
Mo-metal-bpyrim	-	0.6^{o}
W-metal-bpyrim	-	7.1^{o}

The possible path of the electron is designated as a cross-plane path either through the backbone of molecule and this is clear shown in the transmission curve for Bpy and Bpyrim molecules or through metal(CO) group to the end of molecule, and then to the electrodes leads as shown in Figure (3.8).

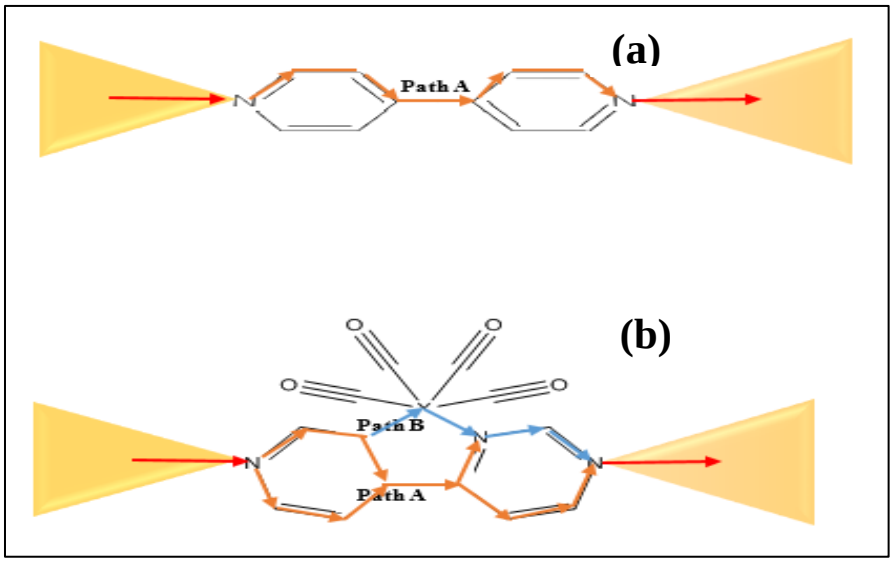

Figure (3.8): Simple carton shows for (a) the electrons path through bpy structure and (b) there are more electrons path through X(CO)4-bpyrim structure.

3.2.4 Binding distance of bipyridine molecule

To calculate the optimum binding distance between pyridyl anchor groups and Au(106) surfaces by using DFT. The binding distance *d* is defined as the distance between the gold surface and the N terminus of the pyridyl group. Here, compound bipyridine is defined as entity A and the gold electrode as entity B. The ground state energy of the total system is calculated using SIESTA and is denoted E_{AB}^{AB}, with the DFT parameters defined as those in the method section of the main text. The gold lead consists of 3 layers of 25 atoms.

The energy of each entity is then calculated in a fixed basis, which is achieved using ghost atoms in SIESTA. Hence, the energy of the individual **2** in the presence of the fixed basis is defined as E_{A}^{AB} and for the gold as E_{B}^{AB}. The binding energy is then calculated using the following equation:

$$\text{Binding Energy} = E_{AB}^{AB} - E_{A}^{AB} - E_{B}^{AB} \qquad \text{…….(3-1)}$$

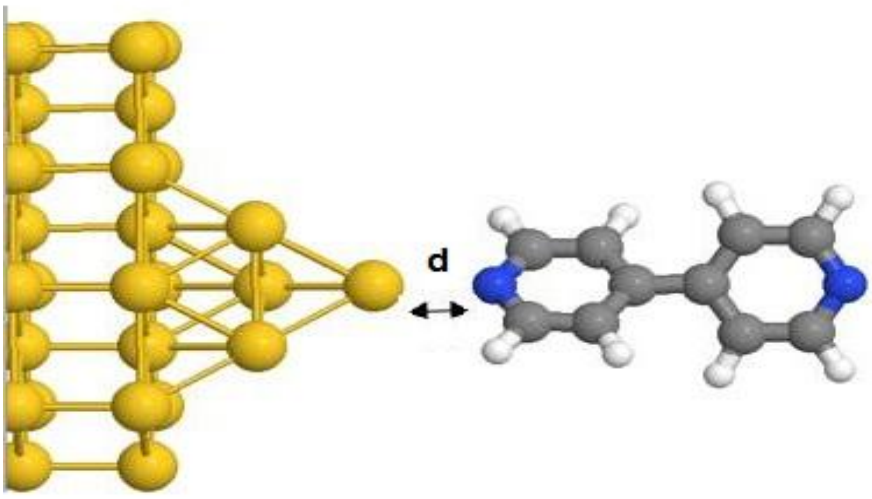

Figure (3.9): shows that for the optimum binding distance *d* is 2.3 Å for bpy molecule and the binding energy is approximately -0.413 (eV).

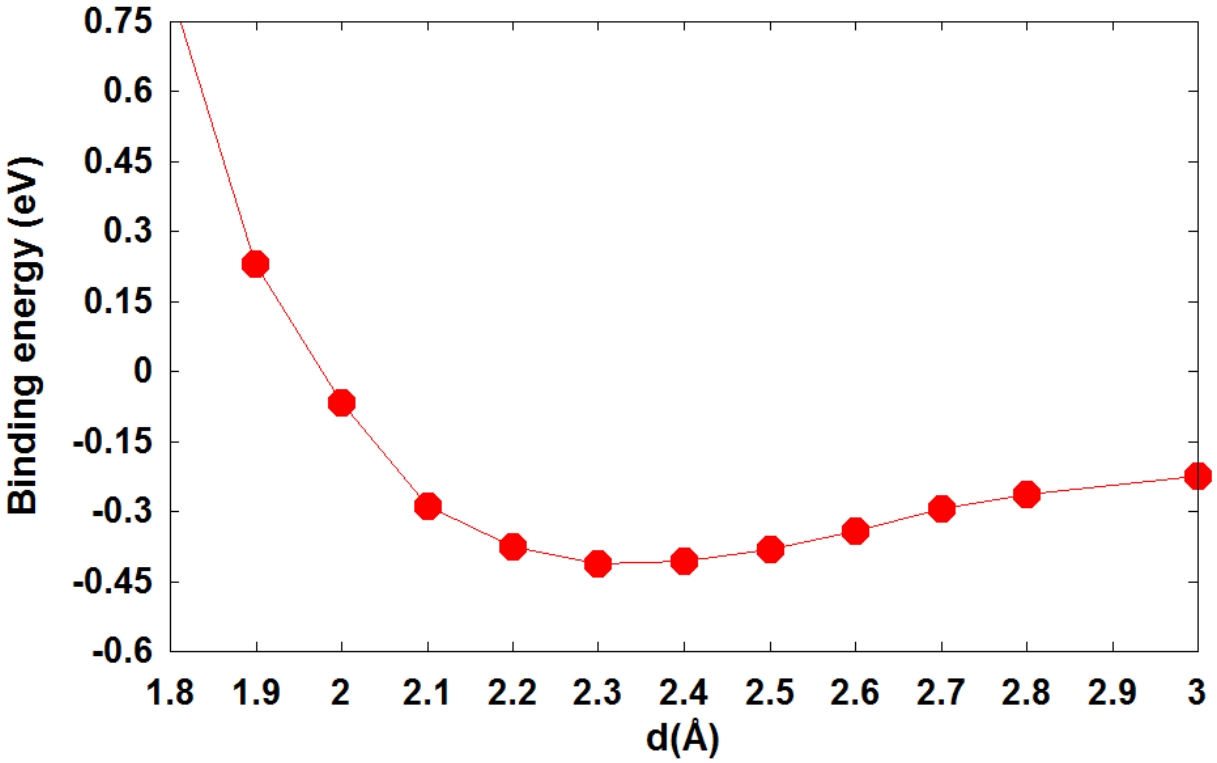

Figure (3.10): Binding energies as a function of the distance (Å) of the nitrogen from the electrode surface.

3.2.5 Transmission Coefficient T(E)

The electrical characteristics were calculated of a family of bipyridine, bipyrimdine, and X(CO)4-bipyrimdine molecules using DFT-based GOLLUM code to compute T(E). Geometrical optimizations have carried out using DFT SIESTA code[101]. All molecules studied in this chapter were freely relaxed in isolation to yield optimized geometries. For each molecular structure, the transmission coefficient of electrons T(E), which describes the propagation of energy of electrons from one electrode to the other was calculated by first calculating the Hamiltonian from SIESTA code, and then using GOLLUM code to compute T(E), electrical conductance was calculated at room temperature using relation (2.45).

The optimized distance between anchor group N and the gold electrodes was 0.23 nm. The transport coefficient, T(E) is characterizing the passage of electrons with energy E from the left to the right electrode for two gold leads, the T(E) coefficient was computed for each relaxed junction structure by first deriving the relevant Hamiltonian and overlap matrices using the DFT-based SIESATA and GOLLUM [103].

To understand more about the thermoelectroics devices, DFT simulations were performed to see how the electrical conductance of molecular structures changes with the type of each molecule under study. As mentioned previously, the *gold lead/**molecule**/gold lead* were linked perpendicularly to the plane of the molecules, and the planar geometries of the molecules were studied.

The mechanics of the transport calculations was represented the transmission coefficients of bipyridine and X(CO)4 bipyrimdine molecules that were appeared various results around Fermi energy E_F as shown: for bipyridine and bipyrimdine molecules without metal complexes, the findings exhibited bipyridine molecule was lower than bipyrimdine about twice as shown in Figures (3.9). This difference is due to the chemical structure between molecules, as well as the effect of the molecular conformation as shown in Figure (3.1a).

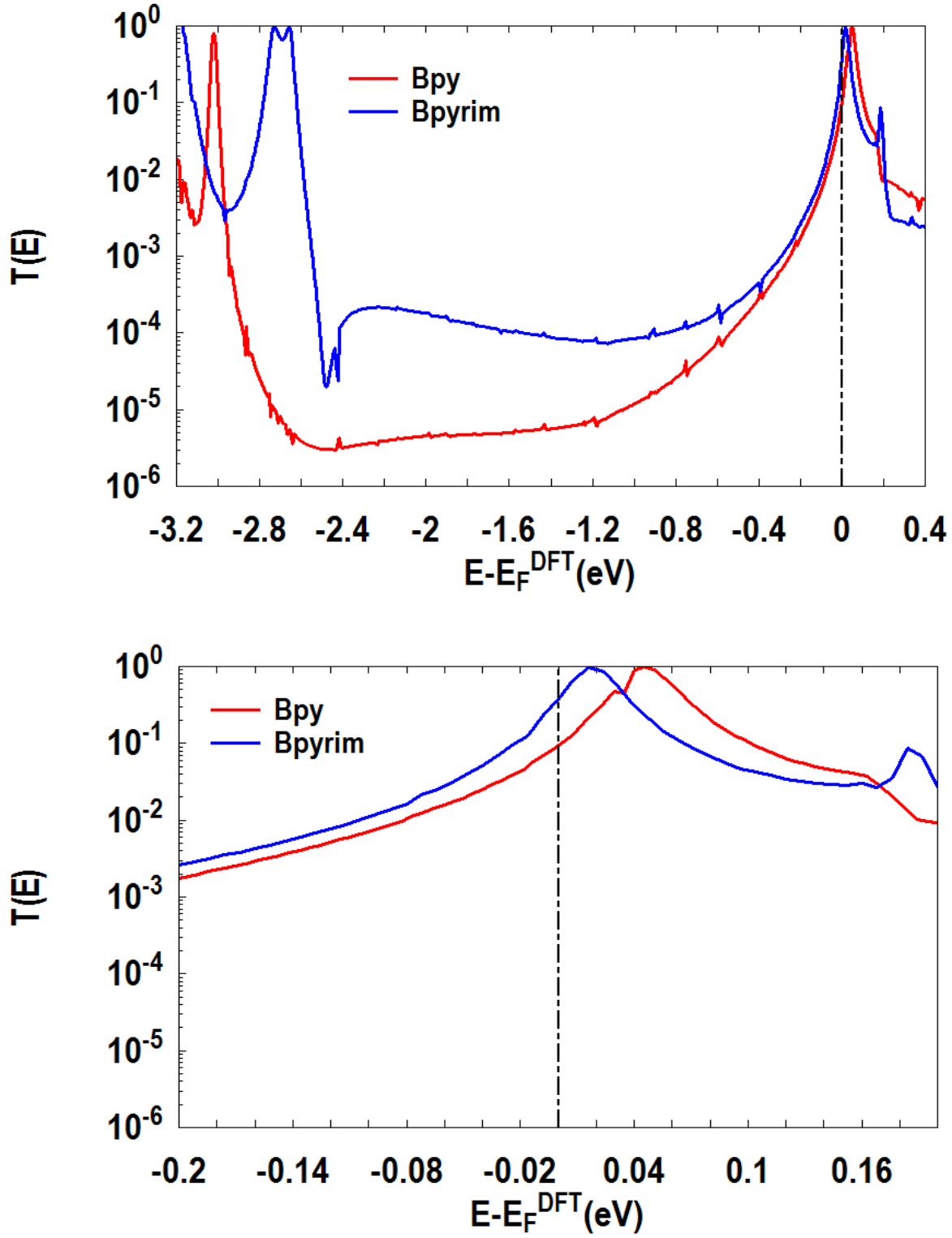

Figure(3.11): Theoretical calculation of transport coefficient as a function of the Fermi energy for Bpy and Bpyrimdine.

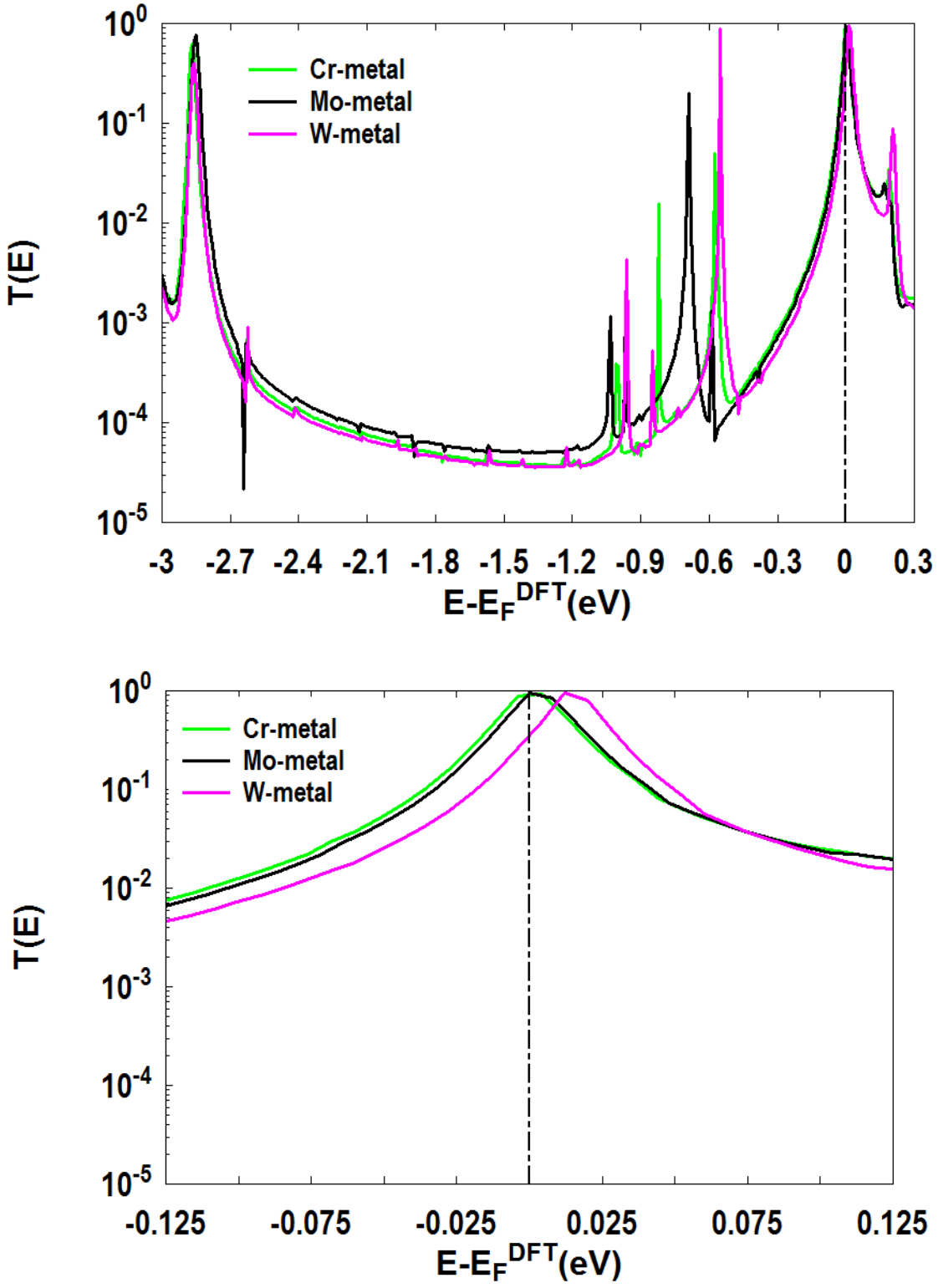

Figure (3.12): Theoretical calculation of transport coefficient as a function of the Fermi energy for X(CO)4-bipyrimdine molecular junctions.

However, to demonstrate the role of the metal-complexes center on the electrical and thermoelectric properties. It can be seen from Figures (3.12) that the magnitude of the transmission coefficient is represented by three curves for each central metal atom presented through HOMO-LUMO energy.

It is clear, that quantum interference appears in those metal complexes structures, which gives importance to present the role of metal-complexes in the route of tunneling. The charge transfer between the metal complexes and backbone molecule is clearly seen in the frontier molecular orbitals (FMO). Furthermore, this corresponds with a recent theoretical study showing the tunneling electron in pyridine structures flows through LUMO energy as demonstrated by the experimental results [110-112]. The electron transport presents that the DFT predicted Fermi energy ($E-E_F=0$ eV) lies near to the LUMO peaks as shown in Figures (3.11 and 3.12). When compared to the transmission peaks of the other molecules such Cr-Mo-W(CO)4 molecules, the transmission peaks were narrow and distinct of organometallic complexes in Figure (3.12).

That means the charge transfer rate between the central metal complex and the backbone of the molecule also contributes to the interactions intensity. In addition, the length of the bond between the central metal atom and the backbone can also be used to get this result. Where we found that the bond length in both was 2.050 Å (N-Cr), 2.086 Å (N-Mo) and was shorter than the bond in (N-W) with > 2.2 Å. As a result, not only the molecular conformation but also the length of the electron transport path can be considered important factors in transmission coefficient variation. The resonance states associated with the various peaks were determined using a projected molecular orbital analysis.

3.2.6 Electrical Conductance

The electrical conductance *G* also was calculated at room temperature using the equation (2.45).To investigate the electrical conductance in more detail, the DFT simulations were performed to examine how the conductance of molecules changes with the energy of Fermi energy as shown in Figures (3.13) where G/G_o is a function of energy.

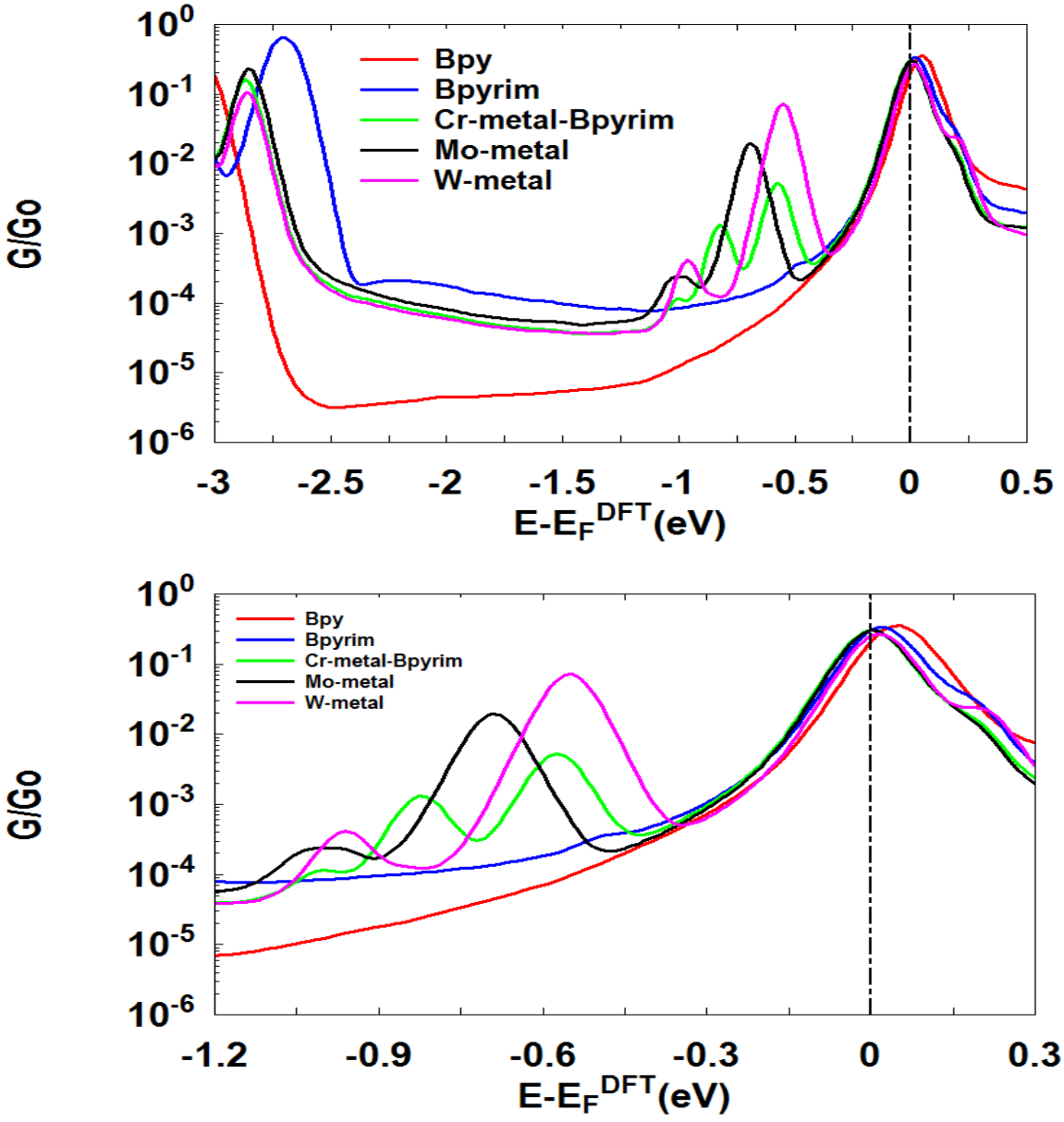

Figure (3.13): Electrical conductance values as a function of energy at room temperature for Bpy (red), Bpyrim (blue), Cr-metal (green), Mo-metal (black), and W-metal (pink).

From Figure (3.13), it is clearly seen that the electrical conductance of five molecules was various values at Fermi energy (E_F), which leads to appear the resonances are close to Fermi energy for Cr, Mo, and W central metal atoms to show the important role of those complexes, in particular the quantum interference concept in single-molecule junctions.

3.2.7 Seebeck Coefficients

Theoretical investigation into the Seebeck coefficient S of molecular junctions using a quantum transport method using Bpy, Bpyrim , Cr-metal, Mo-metal , and W-metal. For the thermoelectric coefficient, the thermoelectric structures will later be used to construct molecular structures. Several molecules have been investigated to understand more about the factors that could the effect the sign and magnitude of their thermopower.

Therefore, when a temperature is differential *T* and a voltage variation *V* through a system, the thermoelectric effect might be characterized as a conversion between thermoelectric and electric energy. This occurs in the passing of an electrical *I* and a heat Q currents via a molecular device. The Seebeck coefficient S was calculated from the relation (2.48) in chapter two. The results were demonstrated in Figure (3.14).

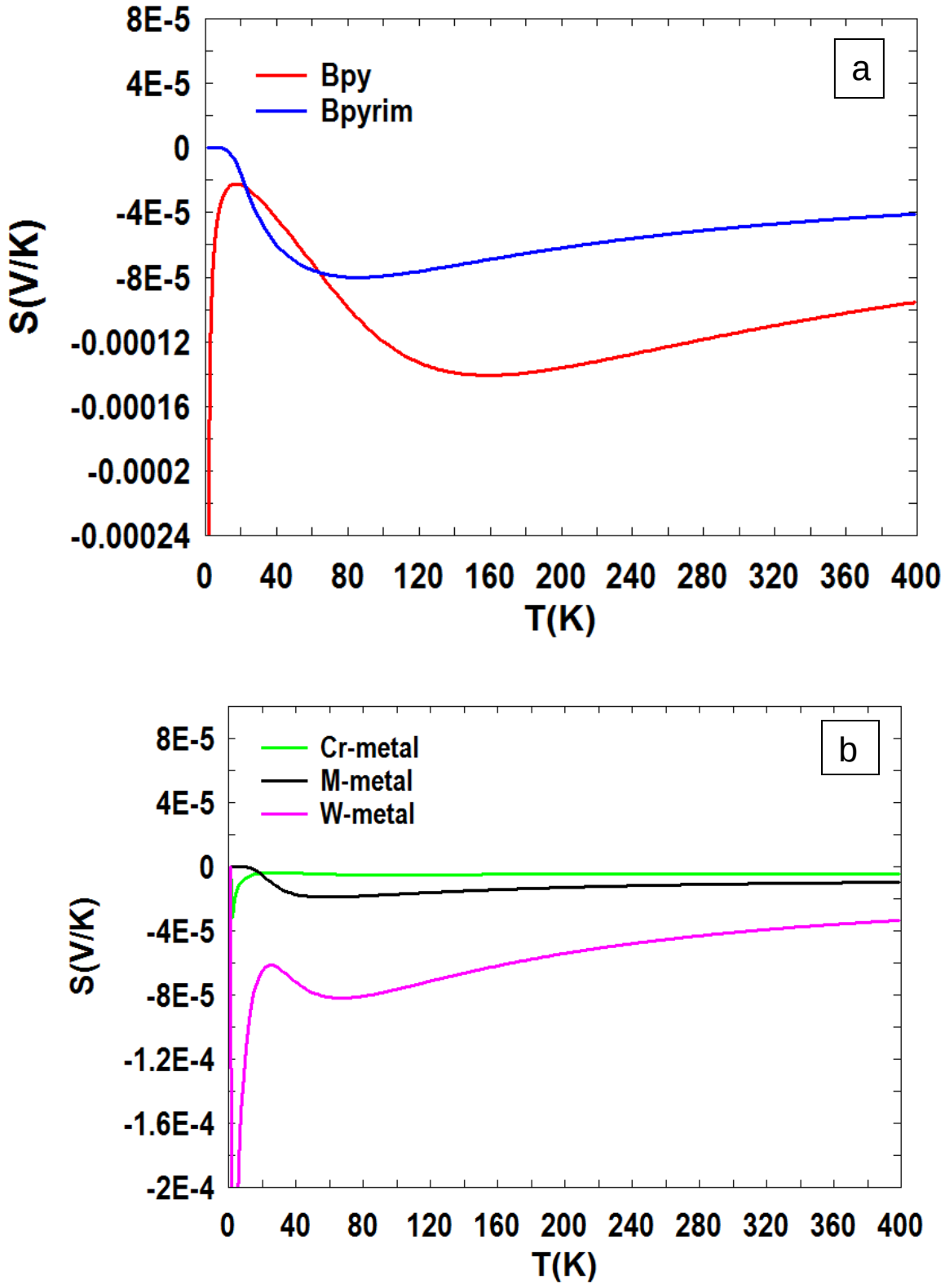

Figure (3.14): Seebeck coefficient S as a function of the temperature for a) Bpy and Bpyrim b) X(CO)4-bipyrimdine molecular junctions at Fermi energy.

It can be shown that quantum interference produces resonances in the gap between the HOMO and LUMO resonances. The shifting of this resonance leads to an enhancement of the thermopower *S*. This behavior is dependent on the connectivity of the molecule as a para-connected molecule produces a constructive feature that dominates and reduces the sensitivity to destructive interference through the pi-orbital geometry.

A more thorough comprehension of thermoelectric properties can be represented by the Seebeck coefficient that clearly shows its behavior at passing the heat current from the hot side to another colder nanowires (organic and organometallic materials) in the presence of complex metals.

In the fact, the change of the sign of thermopower depends on either the connection between the molecular and the electrodes or on the pi-conjugated molecules. Therefore, the transmission coefficient T(E) at the Fermi level E_F provided by DFT is closest to the LUMO resonance, with a positive slope due to the existence of pyridine anchors; however, the Seebeck coefficient is negative, indicating that the LUMO is moving closer to the Fermi energy.

Figure (3.15) shows the value of *S* is proportional to the slope of the transmission at the Fermi Energy. The oscillator of Seebeck coefficient with electron energy of the set molecules that were studied in this thesis. The HUMO-dominated at the DFT Fermi energy leads to the negative Seebeck coefficient. In addition, to demonstrate the oscillated sign of thermopower of metal-complexes molecules (green, black, and pink lines) in Figure (3.15b), hence appears the role of these metals, but all these results are various position and so far from Fermi energy E_F between (-1.173 to-0.28 eV).

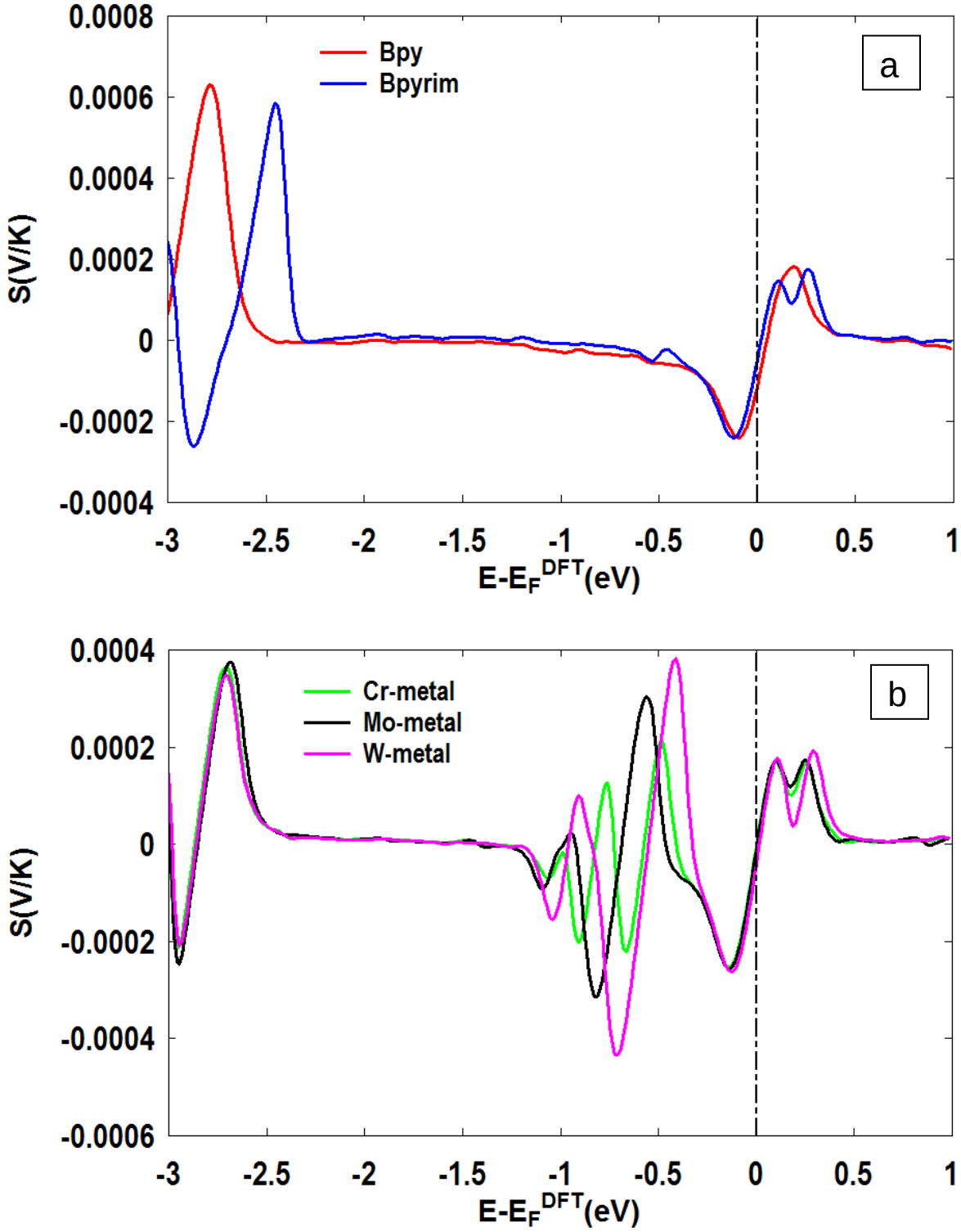

Figure (3.15): Thermopower *S* as a function of electron energy for a) bpy and bpyrim and b) Cr-Mo-W(CO)4 bipyrimdine molecules, respectively.

Table (3.9) compares the theoretical conductance to the Seebeck coefficient derived from the transmission curves.

Table (3.9): Calculated the electrical conductance and Seebeck coefficient of the set studied molecules

Molecules	**G/Go**	**S(V/K)**
Bpy	0.21064	$-11.419*10^{-5}$
Bpyrim	0.30565	$-0.4.897*10^{-5}$
Cr(CO)4-Bpyrim	0.30361	$-0.457*10^{-5}$
Mo(CO)4-Bpyrim	0.30102	$-1.077*10^{-5}$
W(CO)4-Bpyrim	0.25353	$-4.104*10^{-5}$

From Figure (3.16) that shows the variations of the Seebeck coefficient and electrical conductance of the family molecules that the quantum-interference-induced resonances or other features in T(E) with steep slopes around E_F were desired because raising the slope of T(E) when increases Seebeck coefficient shown in Figure (3.16a).

Moreover, when the torsion angle is bigger than 0^o, the electrical conductance decreases with increasing the angle between the pyridine rings as in bpy molecule (40^o). However, for Bpyrim and Cr-Mo-W(CO)4 complexes molecules, the electrical conductance is considerably increased with decreasing the twist angle as shown in Figure (3.16b).

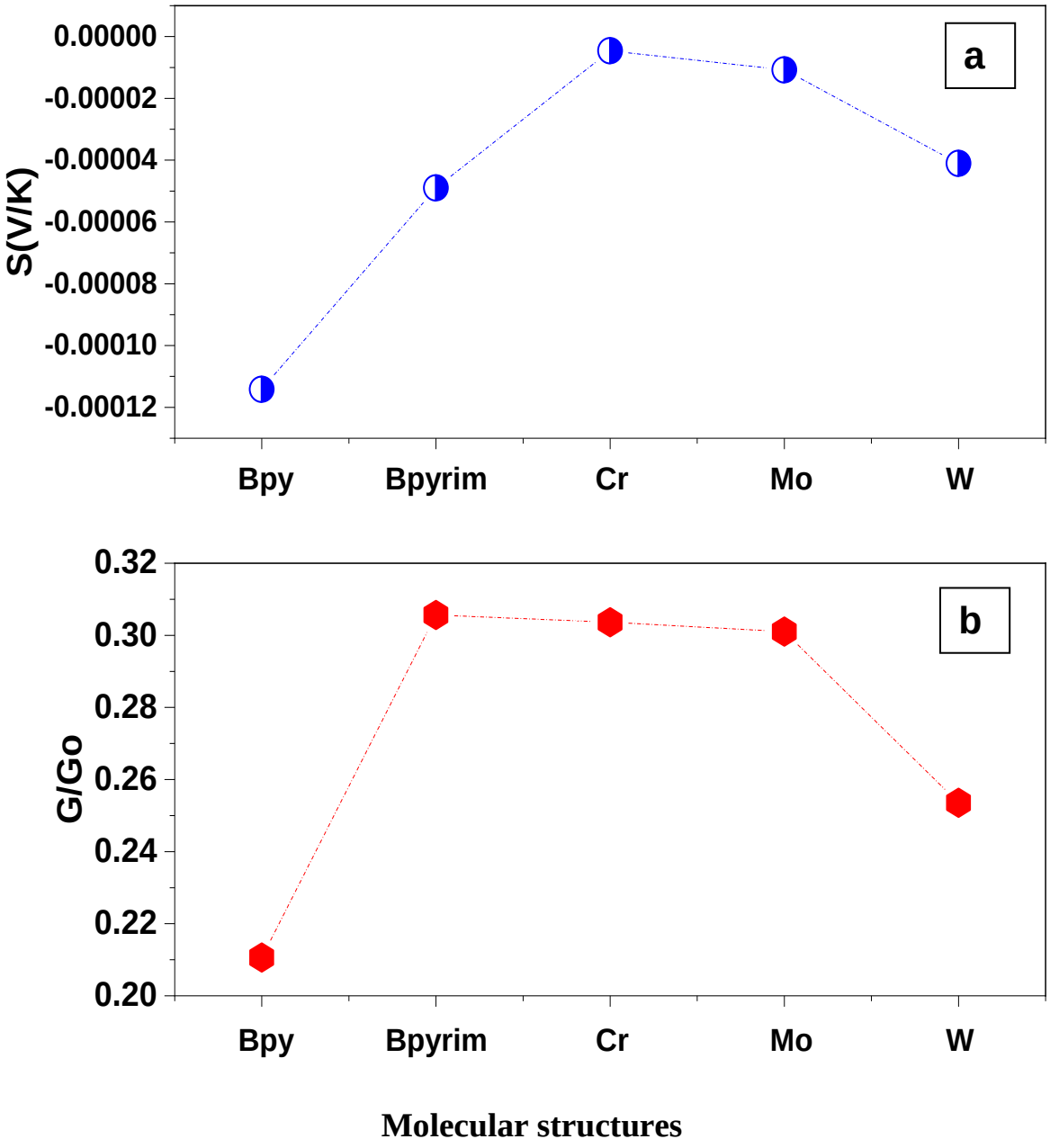

Figure (3.16): Variation of (a) Seebeck coefficient and (b) electrical conductance with the molecular structures at E_F = 0 (eV) the DFT Fermi level.

3.2.8 Figure of Merit (ZT_e)

The electronic contribution to the figure of merit ZT_e at over a range of temperatures has been calculated at Fermi energy E_F as shown in Figures (3.17).

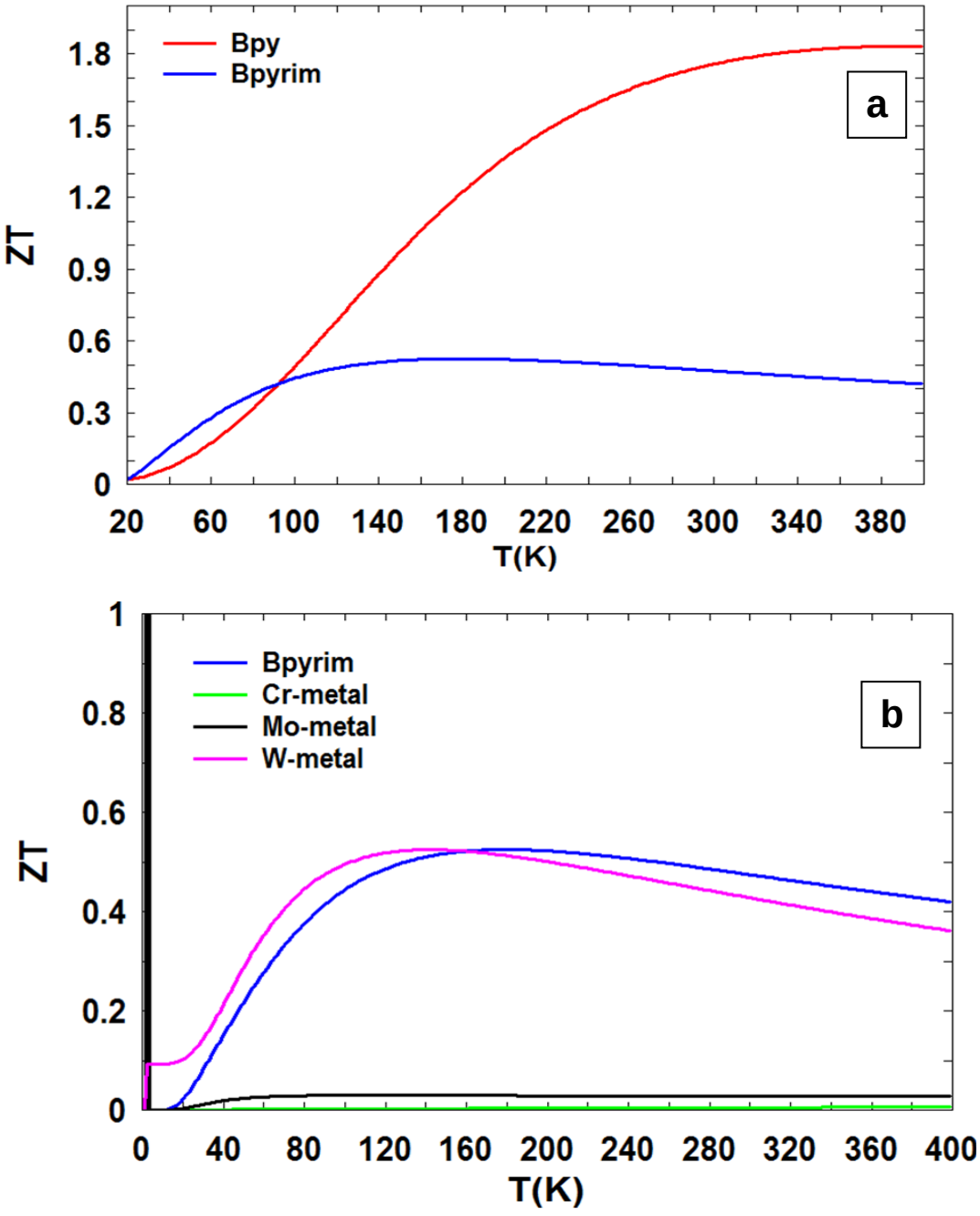

Figure (3. 17): The electronic contribution to the figure of merit ZT_e at Fermi energy as a function of room temperature for a) Bpy and Bpyrim b) central atom (Cr, Mo, and W) metal complexes.

At comparing bpy and bpyrim molecules, the findings were explained the ZT_e value at room temperature of bpy is about 1.75, whereas for bpyrim is 0.474 which means bpy is greater than bpyrim. For metal-complex molecules, it can be shown W metal has a high value compared with other metal complexes as Cr-Mo metal, which have a low value of ZT_e. On the other hand, all these results depend on the position of Fermi energy that limits the value of the figure of merit in all molecular structures used here in this thesis.

From Figure (3.18), as mentioned the ZT_e depodes on the position of the Fermi energy, which determines the values of the electrical conductance and thermppower. Thus, the highest value of ZT_e was for Bpy, whereas the lowest value for Cr-metal-bpyrim molecule. The variation of the value of the figure of merit is due to as mentioned above the chemical structures of those molecules and the position of the Fermi energy.

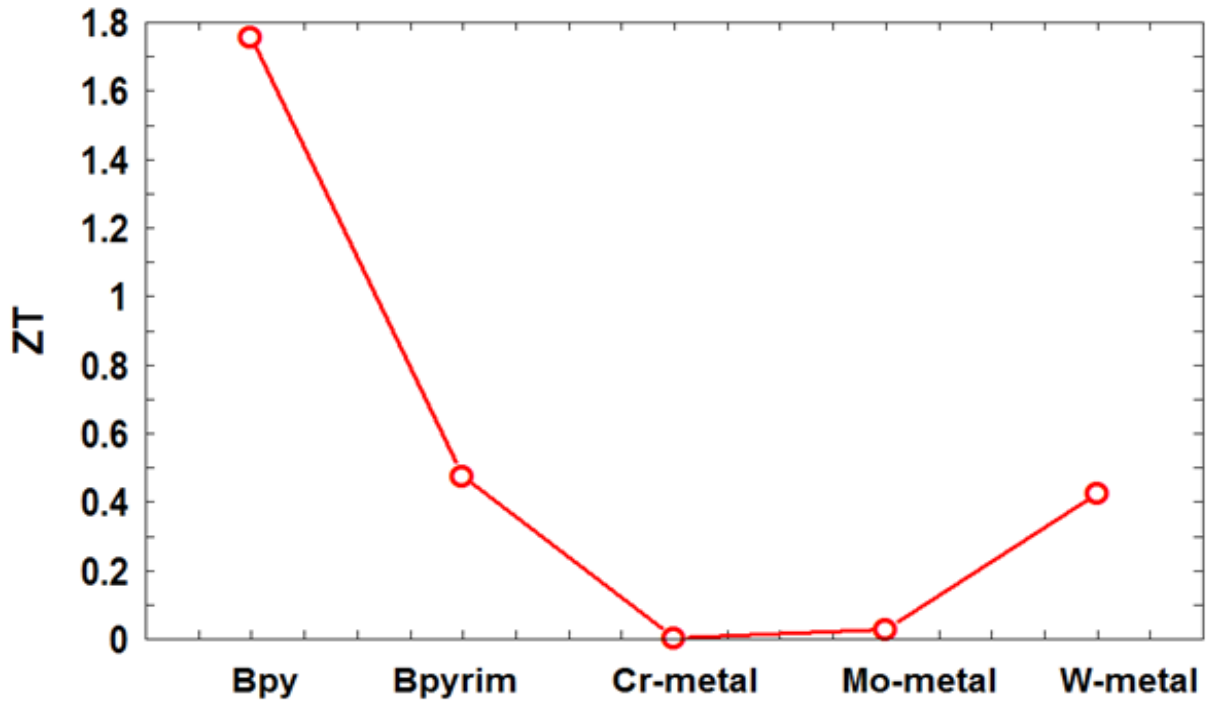

Figure (3.18): the electronic contribution to the figure of merit ZT_e at Fermi energy at room temperature for each central atom (Cr, Mo, and W) metal complexes.

3.2.9 Current–Voltage (I–V) characteristics

To calculate the current-voltage characteristics of those molecules, Figure (3.19) shows the corresponding (I-V) characteristics. To demonstrate the effect of metal complexes on the current-voltage properties, for the first two molecules (Bpy and Bpyrim) the different behavior was exhibited in its curves at a voltage between (-1.6 to 1.6 Volt). The reason behind the difference of (I-V) traces of the voltage ramps is due, as we mentioned before, to the difference in the molecular structure, as well as the torsion angle between the two benzene rings, which led to the emergence of a difference in the value of current and voltage.

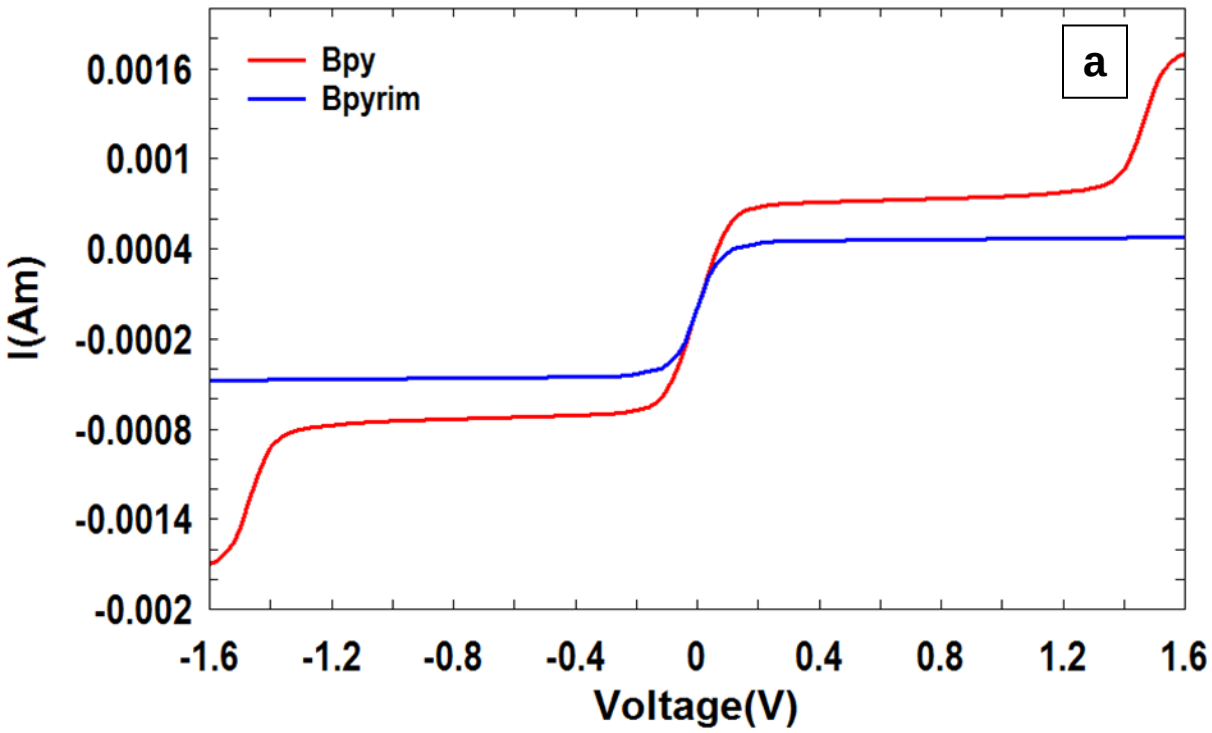

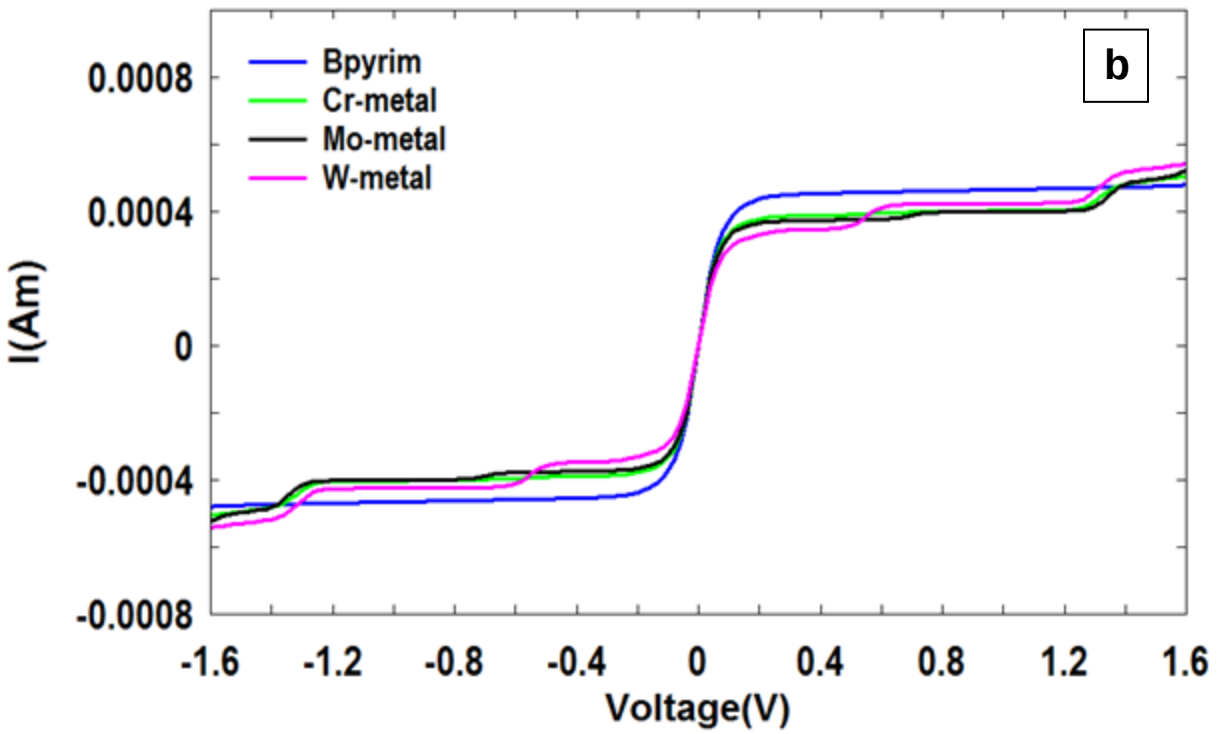

Figure (3.19): The current as a function of voltage at T=300K for a) bpy and bpyrim b) central atom (Cr-Mo-W)-Bpyrim molecules.

The corresponding (I-V) characteristics of each of the complexes were calculated in figure (3.19), as well as the bipyrimdine molecules that contain central metal atoms. It is clear that the bridge between the two pyridine rings, the torsion angle is close to zero, and despite the presence of metal atoms. However, approximately there is no influence for the metal complexes on the (I-V) curve except for W-metal that has slightly different behavior probably associated with the bond lengths between two nitrogen atoms and W-metal and the rest of chemical groups.

Chapter Four

Conclusions and Future works

4.1 Conclusions

In this chapter, it can be summarized all results of various structures as organic and organometallic molecules that have studied through our work to calculate the electronics, electrical and thermal properties of family molecules using Density Function Theory DFT as follows brief conclusions:

1. The findings have exhibited the electronics and optical properties of those molecules improving their applications as industry and Scientific.
2. The metal-ligand chemical bond between metal complexes with CO group and backbone of a molecule plays more important due to change of the absorbance behavior of molecules before and after the addition of these structures, which led to shifts in the absorbance spectrum of the UV-visible with the wavenumber and wavelength, respectively.
3. The results of the electronic properties were interesting due to the decrease in the energy gap, in particular when compared with the bipyridine molecule that used as a basics molecule and X(CO)4-bipyrimdine.
4. The conjugated systems between two pyridel rings is importance in switched and control in electrical, optical, electrical, and thermal properties from their ability to adapt and accommodate their shape, size, and composition.
5. The ordering of transmission coefficient of the studied metal molecules complexes at fermi energy is as Mo > Cr > Bpyrim > W > Bpy.
6. The Seebeck coefficient of all molecules taking advantage of steep slopes depends in transmission coefficient, and the Seebeck coefficients are negative.
7. The Seebeck coefficient is an observable magnitude that is affected by factors such structural conformation, where S in order to as bpy > bpyrim > W > Mo > Cr molecules.

4.2 Future Works

- It would be interesting to look at the role of phonons in thermoelectricity, as well as more exotic types of transport like molecular-scale transport.
- It would be to see how will be changing the thermoelectric results with using other electrodes as platinum or palladium electrodes.
- It will be to use account ion to show the effect of the charge transfer from/ or molecule to account ion.
- To develop our work, it will be using other sides groups or anchor group, which have more effective to increase the electrical and thermal properties.

References

[1] McCreery, R. L. (2004). Molecular electronic junctions. *Chemistry of Materials*, *16*(23), 4477-4496.

[2] Ballhausen, C. J., and Gray, H. B. (1980). *Molecular electronic structures: an introduction*. Benjamin/Cummings Publishing Company.

[3] Mingos, D. M. P., and Dahl, J. P. (Eds.). (2012). *Molecular electronic structures of transition metal complexes II* (Vol. 2). Springer Science & Business Media.

[4] Roco, M., Bainbridge, W., Tonn, B., and Whitesides, G. (2013). Converging knowledge, technology, and society: Beyond convergence of nano-bio-info-cognitive technologies. *Dordrecht, Heidelberg, New York, London*, *450*.

[5] Barish, R. D., Rothemund, P. W., and Winfree, E. (2005). Two computational primitives for algorithmic self-assembly: Copying and counting. *Nano letters*, *5*(12), 2586-2592.

[6] Rakotondrabe, M., Janaideh, M., Bienaim, A., and Xu, Q. (2013). Smart materials-based actuators at the micro/nano-scale. *Characterization, Control and Applications.*

[7] Musa, S. M. (Ed.). (2011). *Computational Nanotechnology: Modeling and Applications with MATLAB®*. CRC Press.

[8] Cuevas, J. C., and Scheer, E. (2010). *Molecular electronics: an introduction to theory and experiment*.q1`

[9] Moore, G. E. (1965). Cramming more components onto integrated circuits.

[10] Bittner, E. R. (2006). Chemical Dynamics in the Condensed Phases: Relaxation, Transfer, and Reactions in Condensed Molecular Systems By Abraham Nitzan (Tel Aviv University). Oxford University Press: Oxford, New York. 2006. xxii+ 720 pp. $89.50. ISBN 0-19-852979-1.

[11] Nitzan, A. (2001). Electron transmission through molecules and molecular interfaces. *Annual review of physical chemistry*, *52*(1), 681-750.

[12] Ratner, M. (2013). A brief history of molecular electronics. *Nature nanotechnology*, *8*(6), 378-381.

[13] Marcus, R. A. (1993). Electron transfer reactions in chemistry. Theory and experiment. *Reviews of Modern Physics*, *65*(3), 599.

[14] Robert, C., Brian, D., Suman, D., Jack, K., Kevin, Z. (2007). Integrated nanoelectronics for the future. *Nature Materials*, 6(11).

[15] Heath, J. R., and Ratner, M. A. (2003). Molecular electronics.

[16] Aradhya, S. V., and Venkataraman, L. (2013). Single-molecule junctions beyond electronic transport. *Nature nanotechnology*, *8*(6).

[17] Pople, J. A., and Beveridge, D. L. (1970). Molecular orbital theory. *C0., NY*.

[18] Streitwieser, A. (2013). Molecular orbital theory for organic chemists. In *Pioneers of Quantum Chemistry*. American Chemical Society.

[19] Mata, R. A., Werner, H. J., and Schütz, M. (2008). Correlation regions within a localized molecular orbital approach. *The Journal of chemical physics*, *128*(14).

[20] Harcourt, R.D. (1999)· Four-Electron Three-Center Bonding: One-Electron and Concerted Two-Electron Delocalization's into Bonding and Antibonding Molecular orbitals. *The Journal of Physical Chemistry*.

[21] Fleming, I. (2011). *Molecular orbitals and organic chemical reactions*. John Wiley & Sons.

[22] Kalsi, P. S. (2000). *Textbook of Organic Chemistry*. Macmillan.

[23] Dryzun, C., Alemany, P., Casanova, D., and Avnir, D. (2011). A continuous symmetry analysis of chemical bonding. *Chemistry-a European Journal*, *17*(22), 6129.

[24] Crabtree, R. H. (2009). *The organometallic chemistry of the transition metals*. John Wiley & Sons.

[25] Crabtree, R. H. (2009). *The organometallic chemistry of the transition metals*. John Wiley & Sons.

[26] Abel, E. W., Labinger, J. A., Labinger, J. A., Stone, F. G. A., Winter, M. J., and Wilkinson, G. (Eds.). (1995). Comprehensive organometallic chemistry II: a review of the literature 1982-1994.

[27] Kaes, C., Katz, A., and Hosseini, M. W. (2000). Bipyridine: the most widely used ligand. A review of molecules comprising at least two 2, 2 '-bipyridine units. *Chemical reviews*, *100*(10).

[28] Constable, E. C., and Housecroft, C. E. (2019). The early years of 2, 2′-bipyridine—a ligand in its own lifetime. *Molecules*, *24*(21).

[29] Li, Z., Smeu, M., Ratner, M. A., and Borguet, E. (2013). Effect of anchoring groups on single molecule charge transport through porphyrins. *The Journal of Physical Chemistry C*, *117*(29), 14890-14898.

[30]Manrique, D. Z., Huang, C., Baghernejad, M., Zhao, X., Al-Owaedi, O. A., Sadeghi, H., and Lambert, C. J. (2015). A quantum circuit rule for interference effects in single-molecule electrical junctions. *Nature communications*, *6*(1), 1-8.

[31] Al-Owaedi, O. A. A. (2016). *Electronic properties of nano and molecular quantum devices*. Lancaster University (United Kingdom).

[32] Al-Galiby, Q. H. H. (2016). *Quantum theory of sensing and thermoelectricity in molecular nanostructures*. Lancaster University (United Kingdom).

[33] Al-Khaykanee, M. K. A. (2018). *Quantum theory of electronic and thermal transport through nano-scale and single-molecule devices*. Lancaster University (United Kingdom).

[34] Naghibi, S., Ismael, A. K., Vezzoli, A., Al-Khaykanee, M. K., Zheng, X., Grace, I. M. and Nichols, R. J. (2019). Synthetic control of

quantum interference by regulating charge on a single atom in heteroaromatic molecular junctions. *The journal of physical chemistry letters*, *10*(20), 6419-6424.

[35] Mutier, M. N., and Al-Badry, L. F. (2020). Electronic and thermoelectric properties of a single pyrene molecule. *Chinese Journal of Physics*, *63*, 365-374.

[36] Yuan, S., Xu, X., Daaoub, A., Fang, C., Cao, W., Chen, H., ... and Hong, W. (2021), Single-atom control of electrical conductance and thermopower through single-cluster junctions. *Nanoscale*.

[37] Al Shareefi, N. M. (2019). Electric Structure of Two Dimensional Molecular Systems. Ph.D. Thesis, College of Science, Babylon University, Iraq.

[38]Griffiths,D.J.(2004). Introduction to Quantum Mechanics (2nd ed.), P rentice Hall, ISBN 0-13-111892-7.

[39] Shankar, R.,(1943). Principles of Quantum Mechanics (2nd ed.)",. Kluwer Academic/Plenum Publishers, ISBN 978-0-306-44790-7.

[40] Mueller, M. P. (2007). *Fundamentals of quantum chemistry: molecular spectroscopy and modern electronic structure computations*. Springer Science & Business Media.

[41] Cox, P. A. (1996). *Introduction to quantum theory and atomic structure*. New York: Oxford University Press.

[42] Fitts, D. D. (1999). *Principles of quantum mechanics: as applied to chemistry and chemical physics*. Cambridge University Press.

[43] Cramer, C. J. (2013). *Essentials of computational chemistry: theories and models*. John Wiley & Sons.

[44] Rogers, D. W. (2003). *Computational Chemistry using the PC*. John Wiley & Sons.

[45] Sahni, V. (2016). Quantal density functional theory. In *Quantal Density Functional Theory* (pp. 67-133). Springer, Berlin, Heidelberg.

[46] Hohenberg, P., and Kohn, W. (1964). Inhomogeneous electron gas. *Physical review*, *136*(3B), B864.

[47] Hameka, H. F. (2004). *Quantum mechanics: a conceptual approach*. John Wiley and Sons.

[48] Lipkowitz, B. K. Larter R., Cundari R. T. and Boyd D. B. (2005) .Reviews in computational chemistry", John Wiley and Sons, Inc., Hoboken, New Jersey.

[49] Hehre, W. Radom L., Schileyer P. and Pople J. (1986) Ab-initio molecular orbital theory, John Wiely and Sons.

[50] Liu, K., Xu, X., Shan, W., Sun, D., Yao, C., and Sun, W. (2020). Study on third-order nonlinear optical properties of the composite films with Ag nanoparticles and CdSe quantum dots. *Optical Materials*, *99*, 109569.

[51] Reimers, J. R. (2011). *Computational methods for large systems: electronic structure approaches for biotechnology and nanotechnology*. John Wiley and Sons.

[52] Parr, R. G., and Yang, W. (1994). Density-functional theory of atoms and molecules. International Series of Monographs on Chemistry. *Oxford University Press, New York*, *3*, 14312-14321.

[53] Kim, K., and Jordan, K. D. (1994). Comparison of density functional and MP2 calculations on the water monomer and dimer. *The Journal of Physical Chemistry*, *98*(40), 10089-10094.

[54] Kose, S., Atay, F., Bilgin, V., and Akyuz, I. (2009). In doped CdO films: Electrical, optical, structural and surface properties. *International journal of hydrogen energy*, *34*(12), 5260-5266.

[55] Callister, W. D., Rethwisch, D. G., Blicblau, A., Bruggeman, K., Cortie, M., Long, J., and Orwa, J. (2021). *Materials science and engineering: an introduction*. wiley.

[56] Liu, X., Chen, S., Li, M., and Wang, X. (2007). Synthesis and characterization of ferromagnetic cobalt-doped tin dioxide thin films. *Thin Solid Films*, *515*(17), 6744-6748.

[57] Martinez, A. I., and Acosta, D. R. (2005). Effect of the fluorine content on the structural and electrical properties of SnO2 and ZnO–SnO2 thin films prepared by spray pyrolysis. *Thin solid films*, *483*(1-2), 107-113.

[58]Matthews P.T., (1974) Introduction to Quantum Mechanics, Mc. Grew-Hill,(1974).

[59] Gotwals, R. R., and Sendlinger, S. C. (2007). A Chemistry Educator's Guide to Molecular Modeling. *The North Carolina School of Science and Mathematics, Durham, NC*.

[60] Dorsett, H., and White, A. (2000). *Overview of molecular modelling and ab initio molecular orbital methods suitable for use with energetic materials*. DEFENCE SCIENCE AND TECHNOLOGY ORGANIZATION SALISBURY (AUSTRALIA).

[61] Gotwals, R. R., and Sendlinger, S. C. (2007). A Chemistry Educator's Guide to Molecular Modeling. *The North Carolina School of Science and Mathematics, Durham, NC*.

[62] Cox, P. A. (1996). *Introduction to quantum theory and atomic structure*. New York: Oxford University Press.

[63] Enkovaara, J., Rostgaard, C., Mortensen, J. J., Chen, J., Dułak, M., Ferrighi, L., and Jacobsen, K. W. (2010). Electronic structure calculations with GPAW: a real-space implementation of the projector augmented-wave method. *Journal of physics: Condensed matter*, *22*(25), 253202.

[64] Xia K., Zwierzycki M., Talanana M., Kelly P. J., and Bauer G., (2006). *Journal of Physical Review* B, Vol.73, PP.1-6,

[65] Hohenberg, P., and Kohn, W. (1964). Inhomogeneous electron gas. *Physical review*, *136*(3B), B864.

[66] C. Zhan, J. Nichols and D. Dixon (2003), *Journal of Physical Chemistry A*, Vol.107, PP.41-84.

[67] Sadasivam, K., and Kumaresan, R. (2011). Theoretical investigation on the antioxidant behavior of chrysoeriol and hispidulin flavonoid compounds–A DFT study. *Computational and Theoretical Chemistry*, *963*(1), 227-235.

[68] Fleming, I. (1976). Frontier Orbitals and Organic Chemical Reactions' John Wiely & Sons. *New York*, *5*.

[69] Kim, B. G. (2010). *Mercury-containing species and carbon dioxide adsorption studies on inorganic compounds using density functional theory*. The University of Arizona.

[70] Naghavi, S. S. (2010). *Theoretical study of correlated systems using hybrid functionals* (Doctoral dissertation, Ph. D. thesis, Mainz University).

[71] Riahi S., Eynollahi S. and Ganjali M., (2009).*Journal of International Electrochemical Science*, Vol.4, PP.11-28

[72] prasad O., Kumar A., Narayan V., Mishra N., Srirastava K. and Sinha L. (2011).*Journal of Chemical and Pharmaceutical Research*, Vol.3, PP.668.

[73] Satar A. (2010) A Spectral and Structural Studies of Cobalt-phthalocyanine (CoPc), Ph.D. Thesis, Al-Mustansiriyah University,

[74] N. Egbedi, I. Obot, M. Khaiary, S. Umoren and E. Ebenso (2011), *Journal of International Electrochemical Science*, Vol.6, PP.5649,.

[75] Sancho-García, J. C., and Pérez-Jiménez, A. J. (2010). A theoretical study of π-stacking tetracene derivatives as promising organic molecular semiconductors. *Chemical Physics Letters*, *499*(1-3), 146-151.

[76] Sert, Y., Ucun, F., El-Hiti, G. A., Smith, K., and Hegazy, A. S. (2016). Spectroscopic Investigations and DFT Calculations on 3-

(Diacetylamino)-2-ethyl-3H-quinazolin-4-one. *Journal of Spectroscopy, Spectroscopy, 2016*.

[77] Oftadeh, M., Naseh, S., and Hamadanian, M. (2011). Electronic properties and dipole polarizability of thiophene and thiophenol derivatives via density functional theory. *Computational and Theoretical Chemistry*, *966*(1-3), 20-25.

[78] Agapito, L. A., and Seminario, J. M. (2007). Metal—molecule—semiconductor junctions: An ab initio analysis. In *Theoretical and Computational Chemistry* (Vol. 17, pp. 1-54). Elsevier.

[79] Hazim, A., Abduljalil, H. M., and Hashim, A. (2020). Analysis of Structural and Electronic Properties of Novel (PMMA/Al 2 O 3, PMMA/Al 2 O 3-Ag, PMMA/ZrO 2, PMMA/ZrO 2-Ag, PMMA-Ag) Nanocomposites for Low Cost Electronics and Optics Applications. *Transactions on Electrical and Electronic Materials*, *21*(1), 48-67.

[80] J. David (1995) Introduction to Quantum Mechanics, 2nd ed. Pearson Education International, America.

[81]MacDonald, D. K. C. (2006). *Thermoelectricity: an introduction to the principles*. Courier Corporation.

[82] Brocks, G. (2005). Electron transport at the nanoscale lecture notes, preliminary version.

[83] Bayin, Ş. S. (2006). Mathematical Methods in Science and Engineering: Bayin/Mathematical.

[84] Zaitsev, V. F., and Polyanin, A. D. (2002). *Handbook of exact solutions for ordinary differential equations*. CRC press.

[85] Polyanin, A. D. (2002). Linear partial differential equations for Engineers and Scientists. *Chapman and*.

[86] Frisch M. J., Trucks G. W., Schlegel H. B., Scuseria G. E., Robb, M. A., Cheeseman J. R., Montgomery J. A., Jr., Vreven T., Kudin K. N.,

Burant J. C., Millam J. M., Iyengar S. S., Tomasi Barone J., Mennucci V., B., Cossi M., Scalmani G., Rega N., Petersson G. A., Nakatsuji H., Hada M., Ehara M., Toyota K., Fukuda R., Hasegawa J., Ishida M., Nakajima T., Honda Y., Kitao O., Nakai H., Klene M., Li X., Knox J. E., Hratchian H. P., Cross J. B., Adamo C., Jaramillo J., Gomperts R., Stratmann R. E., Yazyev O., A Austin. J., Cammi R., Pomelli C., Ochterski J. W., Ayala P. Y., Morokuma K., Voth G. A., Salvador P., Dannenberg J. J., Zakrzewski V. G., Dapprich S., Daniels A. D., Strain M. C., Farkas O., Malick D. K., Rabuck A. D., Raghavachari K., Foresman J. B., Ortiz J. V., Cui Q., Baboul A. G., Clifford S., Cioslowski J., Stefanov B. B., Liu G., Liashenko A., Piskorz P., Komaromi I., Martin R. L., Fox D. J., Keith T., M. Al-Laham A., Peng C. Y., Nanayakkara A., Challacombe M., Gill P. M. W., Johnson B., Chen W., Wong M. W.,and Gonzalez C.,(2009) Gaussian, Inc., Pittsburgh PA,.

[87] Benjamin J. (2005) Lynch, Introduction to GaussView and Gaussian,.

[88] Dennington R., Keith T. and Millam J., (2008) Gauss View 5.0.8, Semichem Inc.

[89] Artacho, E., Gale, J., Garc, A., Junquera, J., and Ordej, P. (2013). D. anchez-Portal and J. *Soler," SIESTA-trunk-462", Fundaci on General Universidad Aut onoma de Madrid*.

[90] Ferrer, J., Lambert, C. J., García-Suárez, V. M., Manrique, D. Z., Visontai, D., Oroszlany, L. and Algharagholy, L. A. (2014). GOLLUM: a next-generation simulation tool for electron, thermal and spin transport. *New Journal of Physics*, *16*(9), 093029.

[91] Rocha, A. R., García-Suárez, V. M., Bailey, S., Lambert, C., Ferrer, J., and Sanvito, S. (2006). Spin and molecular electronics in atomically generated orbital landscapes. *Physical Review B*, *73*(8), 085414.

[92] Pal, S. (2018). *Pyridine: A useful ligand in transition metal complexes* (pp. 57-74). IntechOpen.

[93] Lakshminarayanan, V. (2005). Book Review: Quantum Mechanics: Theory and Applications. By Ajoy K. Ghatak and S. Lokanathan, Kluwer Academic Publishers, Dordrecht, The Netherlands, 2004, xlviii+ 858 pp., $303.00/$99.00 (hardcover/softcover). ISBN 1-4020-1850-9.

[94] Hinker, P., and Hansen, C. (1993, October). Geometric optimization. In *Proceedings Visualization'93* (pp. 189-195). IEEE.

[95] Ismael A. K., Wang K., Vezzoli A., Al-Khaykane M. K., Gallagher H. E., Grace I. M., Lambert C. J., Xu B., Nichols R. J., and Higgins S. J. (2017). Side-Group-Mediated Mechanical Conductance Switching in Molecular Junctions. Angew. Chem. Int. Ed., 56, 15378 –15382.

[96] Grice, K. A., Gu, N. X., Sampson, M. D., and Kubiak, C. P. (2013). Carbon monoxide release catalysed by electron transfer: electrochemical and spectroscopic investigations of [Re (bpy-R)(CO) 4](OTf) complexes relevant to CO 2 reduction. *Dalton Transactions*, *42*(23), 8498-8503.

[97] Al-Khaykanee, M. K., Al-Temimei, F. A., Al-Jobory, A. A., Sabur, D. A., and Abbood, H. I. (2019). Thermoelectric properties of platinum metal complexes. In *AIP Conference Proceedings* (Vol. 2144, No. 1, p. 030020). AIP Publishing LLC.

[98] Soler, J. M., Artacho, E., Gale, J. D., García, A., Junquera, J., Ordejón, P., and Sánchez-Portal, D. (2002). The SIESTA method for ab initio order-N materials simulation. *Journal of Physics: Condensed Matter*, *14*(11), 2745.

[99] Kim, K. S., Tarakeshwar, P., and Lee, J. Y. (2000). Molecular clusters of π-systems: theoretical studies of structures, spectra, and origin of interaction energies. *Chemical reviews*, *100*(11), 4145-4186.

[100] Watson, M. D., Fechtenkötter, A., and Müllen, K. (2001). Big is beautiful−"aromaticity" revisited from the viewpoint of macromolecular

and supramolecular benzene chemistry. *Chemical Reviews*, *101*(5), 1267-1300.

[101] Ferrer, J., Lambert, C. J., García-Suárez, V. M., Manrique, D. Z., Visontai, D., Oroszlany, L., and Algharagholy, L. A. (2014). GOLLUM: a next-generation simulation tool for electron, thermal and spin transport. *New Journal of Physics*, *16*(9), 093029.

[102] Mishchenko, A., Vonlanthen, D., Meded, V., Burkle, M., Li, C., Pobelov, I. V., and Wandlowski, T. (2010). Influence of conformation on conductance of biphenyl-dithiol single-molecule contacts. *Nano letters*, *10*(1), 156-163.

[103] Venkataraman, L., Klare, J. E., Nuckolls, C., Hybertsen, M. S., and Steigerwald, M. L. (2006). Dependence of single-molecule junction conductance on molecular conformation. *Nature*, *442*(7105), 904-907.

[104] Artacho, E., Anglada, E., Diéguez, O., Gale, J. D., García, A., Junquera, J., and Soler, J. M. (2008). The SIESTA method; developments and applicability. *Journal of Physics: Condensed Matter*, *20*(6), 064208.

[105] Finch, C. M., Sirichantaropass, S., Bailey, S. W., Grace, I. M., Garcia-Suarez, V. M., and Lambert, C. J. (2007). Conformation dependence of molecular conductance: chemistry versus geometry. *Journal of Physics: Condensed Matter*, *20*(2), 022203.

[106] Landauer, R. (1957). Spatial variation of currents and fields due to localized scatterers in metallic conduction. *IBM Journal of research and development*, *1*(3), 223-231.

[107] Büttiker, M., Imry, Y., Landauer, R., and Pinhas, S. (1985). Generalized many-channel conductance formula with application to small rings. *Physical Review B*, *31*(10), 6207.

[108] Ie, Y., Hirose, T., Nakamura, H., Kiguchi, M., Takagi, N., Kawai, M., and Aso, Y. (2011). Nature of electron transport by pyridine-based tripodal anchors: potential for robust and conductive single-molecule

junctions with gold electrodes. *Journal of the American Chemical Society*, *133*(9), 3014-3022.

[109] Kamenetska, M., Quek, S. Y., Whalley, A. C., Steigerwald, M. L., Choi, H. J., Louie, S. G., and Venkataraman, L. (2010). Conductance and geometry of pyridine-linked single-molecule junctions. *Journal of the American Chemical Society*, *132*(19), 6817-6821.

[110] Li, R., Hou, S., Zhang, J., Qian, Z., Shen, Z., and Zhao, X. (2006). Analysis on the contribution of molecular orbitals to the conductance of molecular electronic devices. *The Journal of chemical physics*, *125*(19), 194113.

[111] Tan, A., Balachandran, J., Sadat, S., Gavini, V., Dunietz, B. D., Jang, S. Y., and Reddy, P. (2011). Effect of length and contact chemistry on the electronic structure and thermoelectric properties of molecular junctions. *Journal of the American Chemical Society*, *133*(23), 8838-8841.

[112] Al-Khaykanee, M. K., Ismael, A. K., Grace, I., and Lambert, C. J. (2018). Oscillating Seebeck coefficients in π-stacked molecular junctions. *RSC advances*, *8* (44), 24711-24715.

Appendix

Appendix represent the optimized coordinates for atoms in Bipyridine, Bipyrmidine, Cr(CO)4-Bipyrim, Mo(CO)4-Bipyrim, and W(CO)4-Bipyrim respectively.

Appendix (A): Optimized Geometric Parameters (Lengths in Angstrom and Angles in Degree) of Bipyridine.

Atom	X (Å)	Y (Å)	Z (Å)
N	0.001000	0.499600	-3.599900
H	0.011100	-1.571600	-3.479000
H	-0.009100	2.570900	-3.475000
C	0.006500	-0.638100	-2.891700
C	-0.004500	1.636000	-2.889800
C	0.006700	-0.697500	-1.493400
C	-0.004800	1.692700	-1.491600
H	0.011500	-1.680300	-1.491600
H	-0.009600	2.674600	-1.001100
C	0.001000	0.497100	-0.743700
C	0.001000	0.497100	0.743700
H	-1.408500	2.158800	1.000200
H	1.408500	-1.163800	1.005300
C	-0.772100	1. 409800	1.491000
C	0.772100	-0.413700	1.493700
C	-0.735500	1.367100	2.889300
C	0.734500	-0.367900	2.892000
H	-1.340100	2.080500	3.474000
H	1.338100	-1.079700	3.474000
N	-0.001000	0.500400	3.599900

Appendix (B): Optimized Geometric parameters (Lengths in Angstrom and Angles in Degree) of Bipyrimdine.

Atom	X (Å)	Y (Å)	Z (Å)
N	0.000000	0.500000	-3.599900
H	-0.053777	-1.579710	-3.588893
H	0.056257	2.561314	-3.335194
C	-0.041169	-0.676861	-2.955145
C	0.018270	1.588230	-2.815578
C	-0.066460	-0.772915	-1.561219
N	-0.004449	1.634430	-1.480040
H	-0.100102	-1.716758	-0.998719
C	-0.048220	0.442489	-0.858784
C	-0.076588	0.458807	0.622437
H	-0.022676	2.618645	0.772319
N	-0.121444	-0.735425	1.239508
C	-0.057775	1.671450	1.329427
C	-0.145026	-0.695267	2.574731
H	-0.183681	-1.670181	3.090422
H	-0.071646	2.469167	3.359169
N	-0.127139	0.389592	3.363197

Appendix(C): Optimized Geometric parameters (Lengths in Angstrom and Angles in Degree) of Cr(CO)4-Bipyrim.

Atom	X (Å)	Y (Å)	Z (Å)
H	-0.036384	-1.583065	-3.738064
N	0.000000	0.500000	-3.599900
H	0.063128	2.544044	-3.207384
C	0.026355	-0.727911	-3.046601
C	0.076494	1.531278	-2.774117
O	0.215405	5.257802	-2.264443
C	0.126784	-0.917081	-1.669384
C	0.213873	4.411193	-1.460297
N	0.168153	1.479067	-1.418646
H	0.142668	-1.923386	-1.232109
C	0.193941	0.229820	-0.863471
O	-2.853667	3.277728	-0.305126
C	-1.699628	3.199431	-0.206358
Cr	0.203432	3.099556	-0.137846
C	2.104170	3.200480	-0.106787
O	3.261105	3.277020	-0.058822
C	0.280617	0.231100	0.593286
H	0.410790	-1.918700	0.960687
N	0.261547	1.480743	1.149120
C	0.202583	4.410307	1.189691
C	0.385816	-0.913086	1.398892
O	0.220828	5.253453	1.997483
C	0.340864	1.534500	2.505156
C	0.468190	-0.721397	2.777273
H	0.319344	2.546915	2.939176
N	0.445252	0.505855	3.331709
H	0.557301	-1.574122	3.468553

Appendix (D): Optimized Geometric parameters (Lengths in Angstrom and Angles in Degree) of Mo(CO)4-Bipyrim.

Atom	X (Å)	Y (Å)	Z (Å)
H	0.038580	-1.576411	-3.684264
N	0.000000	0.500000	-3.599900
H	-0.030170	2.545408	-3.248182
C	0.040160	-0.708817	-3.016232
C	0.001640	1.546946	-2.800022
O	0.002220	5.412351	-2.491515
C	0.081780	-0.861417	-1.640745
C	0.026610	4.668013	-1.599670
N	0.041210	1.523309	-1.447255
H	0.113920	-1.853139	-1.185885
C	0.082660	0.294706	-0.856929
Mo	0.057090	3.324012	-0.140382
C	2.092630	3.589544	-0.111509
C	-1.979310	3.583790	-0.088763
O	3.208990	3.882421	-0.050692
O	-3.095790	3.880042	-0.047492
C	0.129310	0.298821	0.596153
H	0.211770	-1.846061	0.936230
N	0.112290	1.530446	1.18182
C	0.082000	4.735914	1.253432
C	0.193590	-0.851722	1.386392
O	0.109860	5.551910	2.078417
C	0.157360	1.560901	2.536101
C	0.238650	-0.691913	2.761690
H	0.140870	2.562205	2.978143
N	0.219670	0.518948	3.340744
H	0.292270	-1.555730	3.432506

Appendix (E): Optimized Geometric parameters (Lengths in Angstrom and Angles in Degree) of W(CO)4-Bipyrimine.

Atom	X (Å)	Y (Å)	Z (Å)
H	0.142173	-1.583519	-3.617903
N	0.000000	0.500000	-3.599900
H	-0.135364	2.558098	-3.310708
C	0.076214	-0.692310	-2.974181
C	-0.071226	1.569967	-2.827965
O	-0.424078	5.580305	-2.575604
C	-0.246168	4.817612	-1.710615
C	0.076051	-0.805146	-1.585386
N	-0.066214	1.592060	-1.468472
H	0.147741	-1.785010	-1.097174
C	3.144103	3.779646	-1.031471
O	0.001061	0.381402	-0.836111
C	2.044366	3.611907	-0.702813
W	0.026857	3.462487	-0.234626
C	-2.000206	3.693151	0.150524
O	-3.115107	3.922224	0.374935
C	-0.000003	0.439064	0.626370
H	-0.197193	-1.697418	1.050786
C	0.313894	4.947356	1.107483
N	0.086034	1.694573	1.163016
C	-0.114357	-0.684224	1.463156
O	0.494211	5.792137	1.890773
C	0.057730	1.776508	2.520250
C	-0.145744	-0.463812	2.838639
H	0.133008	2.797548	2.927124
N	-0.060377	0.771409	3.371928
H	-0.249576	-1.300789	3.547035

الخلاصة

التراكيب الجزيئية لسلسلة من المركبات المعدنية لجزيئات bipyrimdine لها مميزات مثيرة للاهتمام في تطبيقات مختلفة مثل الصناعية والعلمية. يلعب الانتقال خلال المعقدات المعدنية في التراكيب الجزيئية دورًا مهمًا في التفاعلات التي تحدث خلال الجسور المعدنية. استخدمت جزيئات bipyrimdine لإظهار تأثير ذرات المعادن على الخواص الإلكترونية والكهربائية والكهروحرارية، وللتعرف على النظام المترافق لاوربيتالات pi في جميع المحاولات قبل / أو بعد استبدال ذرة كربون واحدة بذرات نيتروجين في واحدة أو اثنتين من حلقات pyridine.

استخدمت برامج SIESTA, Gaussian 09 و GOLLUM في حساباتنا. أظهرت النتائج أن فجوة الطاقة للتراكيب المدروسة تقل بشكل ملحوظ مع نوع الذرات المعدنية ، والتي ظهرت في التطبيقات الإلكترونية لاختلاف فجوات طاقة LUMO-HOMO. علاوة على ذلك، أظهرت النتائج ظهور طيف IR و UV-Vis ، اللذان لهما سلوكًا مختلفًا مع نوع المعقدات المعدنية. أكدت النتائج الكهربائية والكهروحرارية تأثير ذرات المركز للمركبات المعدنية في معاملات الانتقال الكهربائي G و القدرة الحرارية S.

ومن خلال موقع طاقة فيومي ($E-E_F=0$ eV)، تم تحديد التوصيلة الكهربائية ومعامل القدرة الحرارية، وبالتالي حددت قيمة معامل الكفاءة الكهروحرارية ZT_e. ولهذا، وجد ان ZT_e ذات قيمة عالية بالنسبة الى الجزيئة الأولى (Bipyrindine) وتساوي 1.7، والتي تعد اعلى بعدة مرات من بقية الجزيئات الأخرى. في حين ان اقل قيمة بالنسبة ZT_e تعود الى ذرة معدن الكروم.

جمهورية العراق

وزارة التعليم العالي والبحث العلمي

جامعة بابـــل

كلية العلـــوم

قسم الفيزيـــاء

تأثير التراكيب العضوية المعدنية للوصلات الجزيئية على الانتقال الكهربائي والحراري

رسالة مقدمة

الى قسم الفيزياء، كلية العلوم، جامعة بابل وهي جزء من متطلبات نيل درجة الماجستير في العلوم/ الفيزياء

من قبل

عايد فاضل مشير **مشعل** (**بكلوريوس علوم فيزياء**/ ٢٠١١)

إشراف

أ.م.د. رواء مزهر عبيد

أ.م.د. محسن كاظم عبد

٢٠٢١ م

١٤٤٣هـ